SMALL-SCALE TESTING OF HIGH BULK CUBICAL AND SPHERICAL NITROGUANIDINE FOR COMPARATIVE EVALUATION

Robert L. McKenney, Jr
Pamela G. Summers, Capt, USAF
Paul R. Schomber, Capt, USAF
Steven D. Whitney, 1Lt, USAF

REPORT DOCUMENTATION PAGE

Form Approved
OMB No. 0704-0188

1. AGENCY USE ONLY (Leave blank)	2. REPORT DATE	3. REPORT TYPE AND DATES COVERED
	February 91	Interim 5 Sep 88 - 31 Oct 90

4. TITLE AND SUBTITLE
Small-Scale Testing of High Bulk Cubical and Spherical Nitroguanidine for Comparative Evaluation

5. FUNDING NUMBERS
PE. 65130D
PR. ARMD
TA. GX
WU. 32

6. AUTHOR(S)
Robert L. McKenney, Jr.; Pamela G. Summers, Capt, USAF; Paul R. Schomber, Capt, USAF, and Steven D. Whitney, 1Lt, USAF

7. PERFORMING ORGANIZATION NAME(S) AND ADDRESS(ES)
Energetic Materials Branch
Munitions Division
Armament Directorate
Eglin Air Force Base, Florida 32542-5434

8. PERFORMING ORGANIZATION REPORT NUMBER

9. SPONSORING/MONITORING AGENCY NAME(S) AND ADDRESS(ES)
Energetic Materials Branch
Munitions Division
Armament Directorate
Eglin Air Force Base, Florida 32542-5434

10. SPONSORING/MONITORING AGENCY REPORT NUMBER
WL/MN/TR-91-44

11. SUPPLEMENTARY NOTES
This report contains no proprietary data. This report was not edited by the Technical Report Section.

12a. DISTRIBUTION/AVAILABILITY STATEMENT
Approved for public release; distribution is unlimited.

12b. DISTRIBUTION CODE

13. ABSTRACT *(Maximum 200 words)*
Two types of nitroguanidine (NQ), high bulk cubical (HBCNQ) and spherical (SNQ), were tested neat and as melt cast formulations with TNT and with RDX. The objective was to characterize both types of NQ with respect to thermal stability, shock sensitivity and performance. Parameters investigated were thermal stability, critical diameter, detonation velocity and pressure, shock sensitivity, and bullet impact. DSC thermograms from neat HBCNQ and SNQ suggest the former is less stable than the latter. This conclusion is reflected in the apparent activation energies, where that for HBCNQ is about 10 Kcal/mole less than that for SNQ. It is supported by DSC and slow cookoff data from both melt cast formulations. Critical diameters were determined and insight gained into the relationship of charge diameter with that diameter above which the NQ detonation velocity approaches ideal. Shock sensitivities and detonation pressures were obtained. The overall results suggest that ideal performance can be achieved more readily from a formulation with SNQ than with HBCNQ.

14. SUBJECT TERMS	15. NUMBER OF PAGES
Nitroguanidine, spherical nitroguanidine, high bulk cubical nitroguanidine, comparative small-scale testing, explosive performance, melt cast formulations, thermal stability, shock sensitivity	89
	16. PRICE CODE

17. SECURITY CLASSIFICATION OF REPORT	18. SECURITY CLASSIFICATION OF THIS PAGE	19. SECURITY CLASSIFICATION OF ABSTRACT	20. LIMITATION OF ABSTRACT
UNCLASSIFIED	UNCLASSIFIED	UNCLASSIFIED	SAR

PREFACE

This program was conducted by the Energetic Materials Branch (MNE), Munitions Division (MN), Air Force Armament Laboratory (AFATL), Eglin Air Force Base, Florida 32542-5434, under Project ARMDGX32. Capt Pamela Summers and 1Lt Steven Whitney managed the program for the Armament Laboratory and Dr Robert McKenney, Jr., reduced the data and documented the findings and conclusions. The program was conducted during the period from 5 September 1988 to 31 October 1990.

Appreciation is extended to Messrs Gary H. Parsons, Thomas G. Floyd, Stephen A. Aubert, and Dr Michael A. Patrick for their helpful discussions and technical critique regarding this work. Thanks are also extended to Ms Elizabeth A. Deibler for her untiring effort in carrying out a portion of the experimental effort.

TABLE OF CONTENTS

Section	Title	Page
I	INTRODUCTION.	1
II	PROCEDURES.	7
	1. Differential Scanning Calorimetry (DSC) . . .	7
	2. Critical Diameter	7
	3. Detonation Velocity/Pressure.	9
	4. Shock Sensitivity	9
	5. Slow Cookoff (Generic Hardware)	11
	6. Slow Cookoff (SCO Units).	14
	7. Bullet Impact	14
	8. Density	16
III	RESULTS	17
	1. Differential Scanning Calorimetry (DSC) . . .	17
	2. Critical Diameter	30
	3. Detonation Velocity/Pressure.	30
	4. Shock Sensitivity	30
	5. Slow Cookoff (Generic Hardware)	41
	6. Slow Cookoff (SCO Units).	49
	7. Bullet Impact	49
IV	DISCUSSION.	53
V	CONCLUSIONS	75

LIST OF FIGURES

Figure	Title	Page
1	Scanning Electron Micrographs of HBCNQ (146X) and SNQ (200X)	2
2	Scanning Electron Micrographs of HBCNQ (800X) and SNQ (1220X)	3
3	a. Scanning Electron Micrograph of a Fractured SNQ Spherulite Embedded in TNT. b. Scanning Electron Micrograph (Derivative Signal Processing Technique) Showing Spherulite Surface Wetting by TNT	4/5
4	Schematic of a Conical Test Fixture for Measuring Critical Diameters of Explosives.	8
5	Schematic of a Test Fixture for Measuring Plate Dent and Detonation Velocities of Explosives. . . .	10
6	Schematic of Modified ELSGT Configuration	12
7	Schematic of Slow Cookoff Test Apparatus Using Generic Hardware.	13
8	Schematic of a Small-Scale Cookoff Bomb (SCB) Unit.	15
9	DSC Thermogram of HBCNQ (297-420 u)	18
10	DSC Thermogram of HBCNQ (105-210 u)	19
11	DSC Thermogram of SNQ (297-420 u)	20
12	DSC Thermogram of SNQ (105-210 u)	21
13	DSC Thermogram of TNT	22
14	DSC Thermogram of TNT/HBCNQ (297-420 u)	23
15	DSC Thermogram of TNT/HBCNQ (105-210 u)	24
16	DSC Thermogram of TNT/SNQ (297-420 u)	25
17	DSC Thermogram of TNT/SNQ (105-210 u)	26

LIST OF FIGURES (CONT'D)

18	DSC Thermogram of RDX/HBCNQ (210-297 u)	27
19	DSC Thermogram of RDX/SNQ (210-297 u)	28
20	Critical Diameter Pin Data for TNT/SNQ (297-420 u).	31
21	Critical Diameter Pin Data for TNT/HBCNQ (297-420 u).	32
22	Critical Diameter Pin Data for TNT/SNQ (105-210 u).	33
23	Critical Diameter Pin Data for TNT/HBCNQ (105-210 u).	34
24	Critical Diameter Pin Data for RDX/HBCNQ (210-297 u).	35
25	Modified ELSGT Results for TNT/HBCNQ (297-420 u). .	39
26	Modified ELSGT Results for TNT/SNQ (297-420 u). . .	40
27	Modified ELSGT Results for TNT/HBCNQ (105-210 u). .	43
28	Modified ELSGT Results for TNT/SNQ (105-210 u). . .	44
29	Modified ELSGT Results for RDX/HBCNQ (210-297 u). .	46
30	Modified ELSGT Results for RDX/SNQ (210-297 u). . .	47
31	Calculated D(NQ) from Critical Diameter Experiments at a Diameter of 50.8 mm.	55
32	D(NQ) Versus Density for 50.8 mm Diameter Unconfined Cylindrical Charges	58
33	D(NQ) Versus Density for 25.4 mm Diameter Unconfined Cylindrical Charges	59
34	D(NQ) Versus Density for 19.05 and 38.1 mm Diameter Unconfined Cylindrical Charges.	60
35	D(NQ) Versus Density for ELSGT Charges Achieving Constant Velocity Detonation.	66

LIST OF FIGURES (CONT'D)

36 a. Scanning Electron Micrograph (254X) of Internal Porosity Located in an SNQ Spherulite. b. Scanning Electron Micrograph (680X) of Internal Porosity Located in an SNQ Spherulite. 77/78

37 Scanning Electron Micrograph of Large Surface Void Located on an SNQ Spherulite. 79

LIST OF TABLES

Table	Title	Page
1	Activation Energies for HBCNQ, SNQ and the TNT- and RDX-Based Formulations.	29
2	Critical Diameter and Detonation Velocities for TNT- and RDX-Based NQ Formulations.	36
3	Detonation Velocity/Pressure Test Data Summary (295 kbar Input Pressure)	37
4	Modified ELSGT Results for TNT/NQ Melt Cast Systems (297-420 micron NQ)	38
5	Modified ELSGT Results for TNT/NQ Melt Cast Systems (105-210 micron NQ)	42
6	Modified ELSGT Results for RDX/NQ Melt Cast Systems	45
7	Slow Cookoff (Generic Hardware) Test Results.	48
8	Slow Cookoff Test Results (SCO Units)	50
9	Definition of Reactions Seen in SCO Tests	51
10	Bullet Impact Test Results.	52
11	Critical Diameter Data From Cone and Detonation Velocity/Pressure Tests	57
12	Relationship of D(NQ) to Observed Detonation Velocities for TNT/NQ Formulations.	65
13	Relationship of D(NQ) to Observed Detonation Velocities for RDX/NQ Formulations.	68
14	Relationship of D(NQ) to Observed Detonation Velocities for RDX/NQ Formulations from Eight-Inch Gap Experiments	70

SECTION I

INTRODUCTION

Nitroguanidine (NQ) is a commercially available energetic material in the form of flexible needles (α - polymorph), having a bulk (packing) density generally between 0.2 to 0.3 g/cm^3. This crystal habit limits its usefulness as an explosive ingredient primarily because of poor processability characteristics and, less importantly, because of its inherent lower particle density (1.64 $\pm$ 0.03 g/cm^3). The crystal density of NQ is 1.775 g/cm^3. The use of crystal habit modifiers and special recrystallization techniques allow the crystal habit to be changed to forms of higher bulk and particle densities and improved processability characteristics. This report describes the results of an investigation involving two crystalline forms of NQ, herein named high bulk cubical (HBCNQ) and spherical (SNQ). The former is recrystallized from water, and the latter by a special process from dimethylformamide. The sources of the two NQs are the Naval Ordnance Station, Indian Head, Maryland and Fraunhofer-Institut fur Chemische Technologie (ICT) of the Federal Republic of Germany, respectively.

HBCNQ is an irregularly shaped, polyhedral-like particle with as-received bulk and particle densities of 0.948 and 1.760 $\pm$ 0.008 g/cm^3. SNQ, on the other hand, is an example of spherulitic crystallization with radial internal growth structure. The bulk and particle densities for as-received SNQ are 0.976 and 1.724 $\pm$ 0.009 g/cm^3, respectively. Scanning electron micrographs of NQ in the two crystalline habits, HBCNQ and SNQ, are shown in Figures 1 and 2. The former figure gives a general view of a typical particle of each type of NQ and the latter a close-up of the contrasting surface structures. A typical view of the internal structure of a fractured spherulite embedded in a TNT matrix is shown in Figure 3a. Wetting of the outside surface of the spherulite by the TNT is also obvious from this micrograph. Surface wetting of the spherulite surface is better depicted by the derivative signal processing technique shown in Figure 3b. The SNQ-TNT

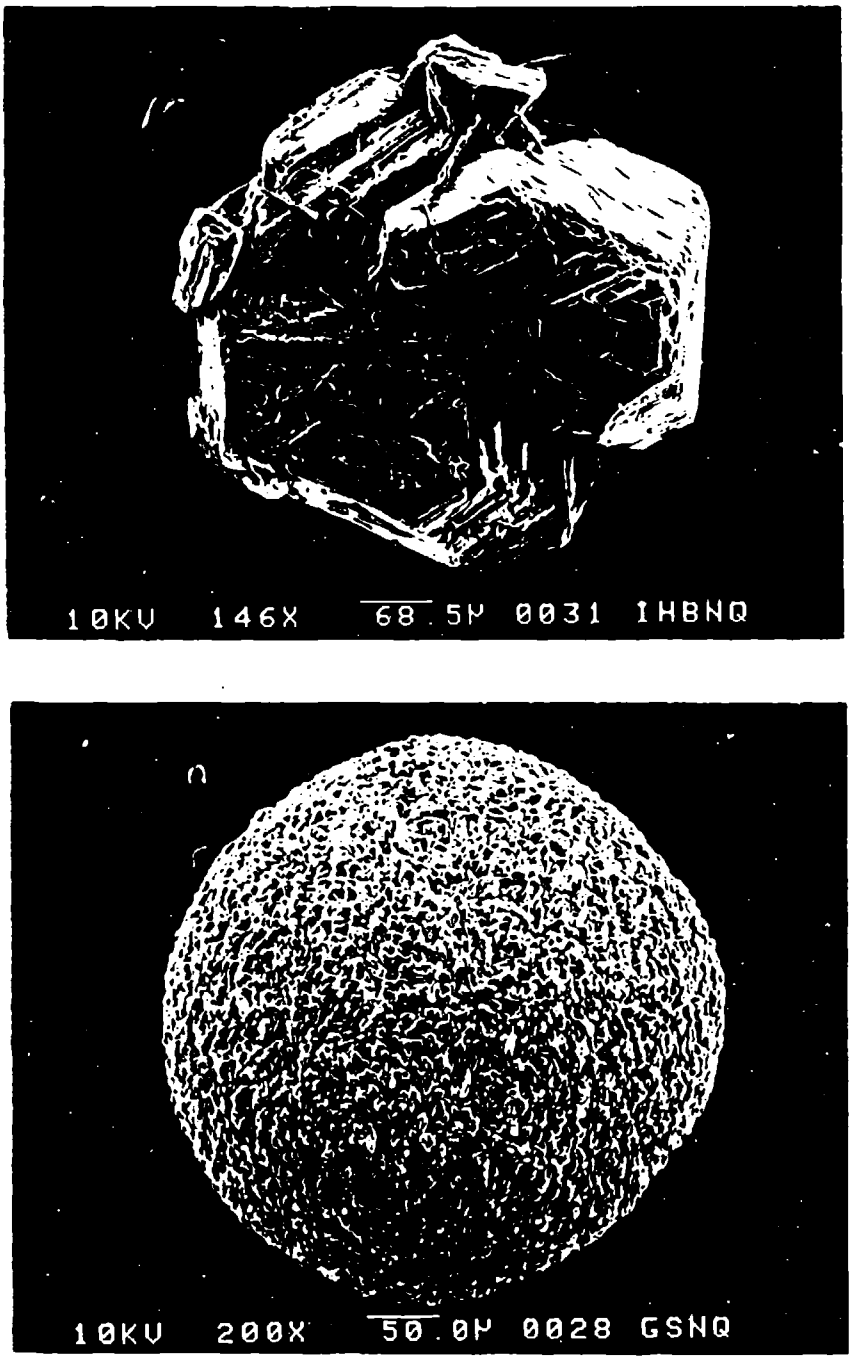

Figure 1. Scanning Electron Micrographs of HBCNQ (146X) and SNQ (200X)

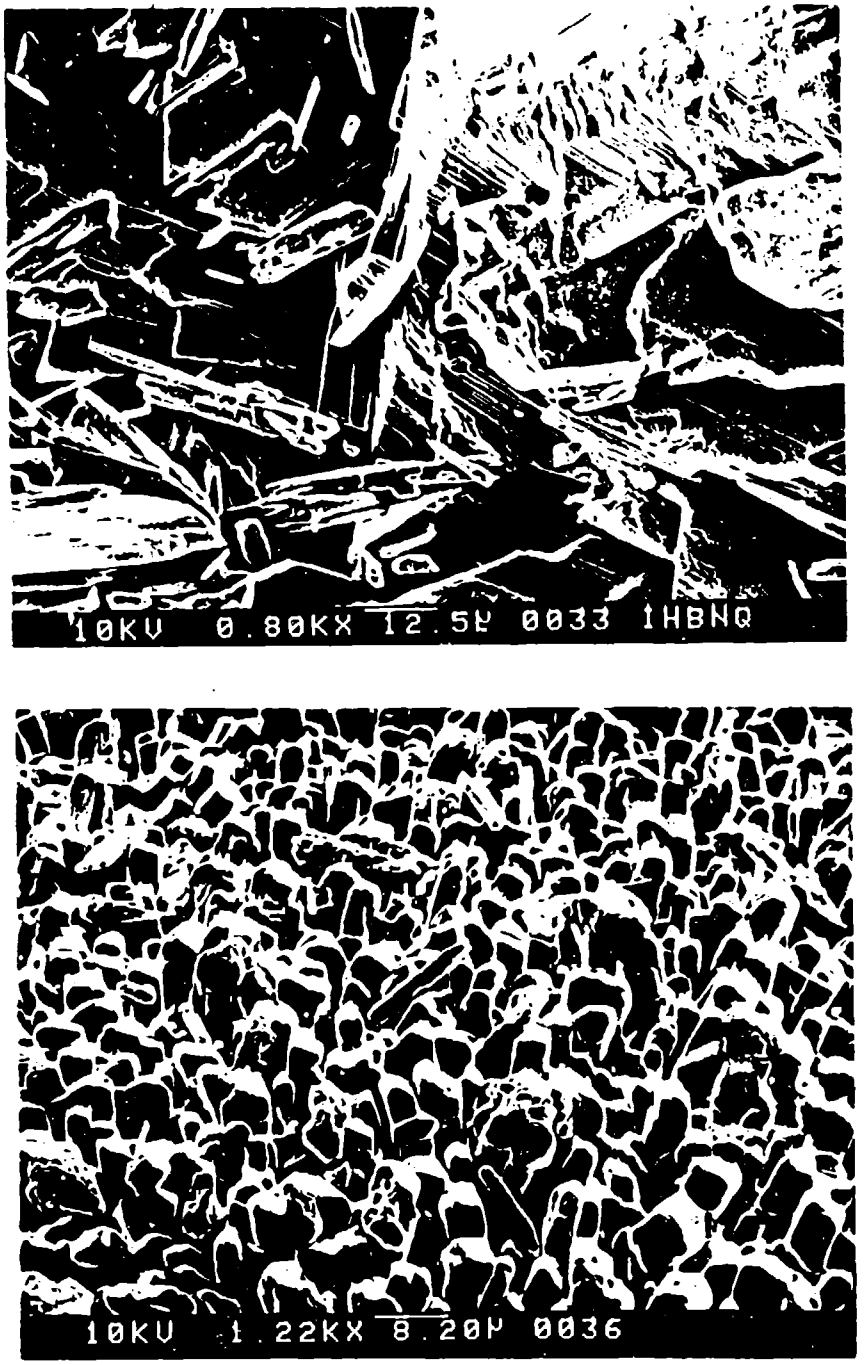

Figure 2. Scanning Electron Micrographs of HBCNQ (800X) and SNQ (1220X)

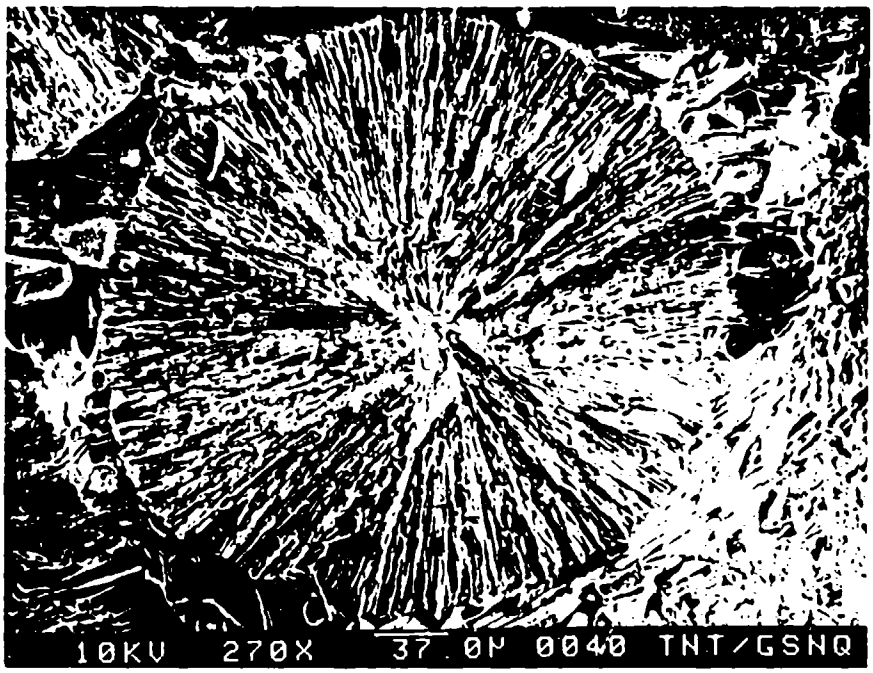

Figure 3.a. Scanning Electron Micrograph of a Fractured SNQ Spherulite Embedded in TNT.

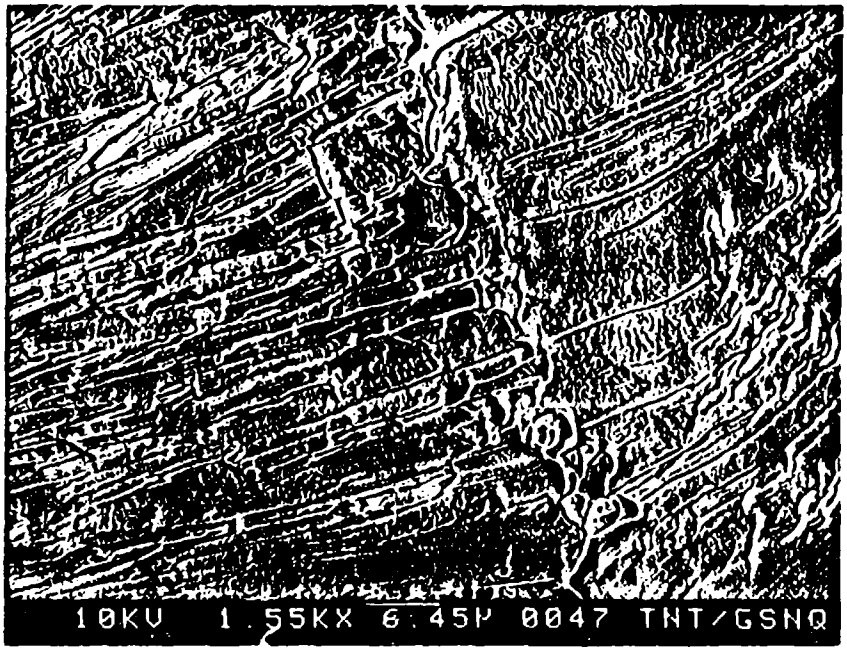

Figure 3.b. Scanning Electron Micrograph (Derivative Signal Processing Technique) Showing Spherulite Surface Wetting by TNT

interface occurs at the center (SNQ on the left and TNT on the right) of the upper boundary of the micrograph and proceeds diagonally from left to right until it intersects the lower boundary two-thirds of the distance from the left boundary.

The two types of NQ were investigated neat and as melt cast formulations with TNT and with RDX as the more sensitive energetic ingredients. Three particle size ranges (105-210, 210-297, and 297-420 microns) were used for each type of NQ. The TNT-based formulations consisted of 50 percent by weight NQ with the remainder TNT. Homogeneous dispersion of the NQ was insured by creaming the TNT during the formulating process. The RDX-based formulations consisted of RDX (21.6 percent), NQ (47 percent), aluminum (17 percent), polywax/DOA (14.1 percent) and lecithin (0.3 percent). The Class E RDX was coated with 10 percent dioctyl adipate (DOA). The aluminum used in the formulation was atomized powder No. 1401 produced by Aluminum Company of America, Rockdale TX, and the wax was Polywax (500) Polyethylenes produced by Petrolite Specialty Polymers Group, Tulsa OK. All percentages are by weight.

The objective of this investigation was to characterize both types of NQ with respect to thermal stability, shock sensitivity, and performance. The parameters chosen were thermal stability by differential scanning calorimetry and slow cookoff characteristics, critical diameter, detonation velocity and pressure, shock sensitivity (gap technique) and bullet impact.

SECTION II

PROCEDURES

1. DIFFERENTIAL SCANNING CALORIMETRY (DSC)

This comparative evaluation was carried out using a Perkin-Elmer DSC-4/Thermal Analysis Data Station System. Apparent activation energies for the thermal decomposition process were obtained using the variable heating rate technique (Reference 1). Large volume, sealed, stainless steel sample capsules (Perkin-Elmer Part No. 0319-0029) were used to insure neither sample ingredients nor decomposition gases were lost during the heating process. Heating rates of 2, 5, 10, 20, and 40°C/minute were used with three experiments being carried out at each heating rate.

2. CRITICAL DIAMETER

Critical diameter determinations were made using a cone of explosive tapering from a diameter of 76.2 mm to 19.05 mm over a length of 330.2 mm. A cylindrical section, 152.4 mm long by 76.2 mm diameter, precedes the tapered portion of the cone to insure steady state detonation is achieved prior to the tapered section. The cone was instrumented with 23 piezoelectric pins spaced 15 mm apart along the length of the tapered section. The booster assembly consisted of an RP2 detonator, a 25.4 mm diameter by 25.4 mm long cylinder of Composition A-5, a 101.6 mm diameter by 50.8 mm long cylinder of Composition C-4 and a 101.6 mm diameter by 50.8 mm long cylinder of Composition B. The latter component of the booster assembly was mounted against the cylindrical section of the experimental cone in a horizontal test configuration. See Figure 4.

The cone test was designed to semi-quantitatively measure the effect of decreasing charge radius on the detonation velocity of a given energetic material or mixture of materials. The use of a conical, as opposed to a cylindrical charge and piezoelectric pins, as opposed to a streak record, results in a degree of uncertainty in the actual location of the critical diameter. In fact, critical diameter values for ideal explosives using the

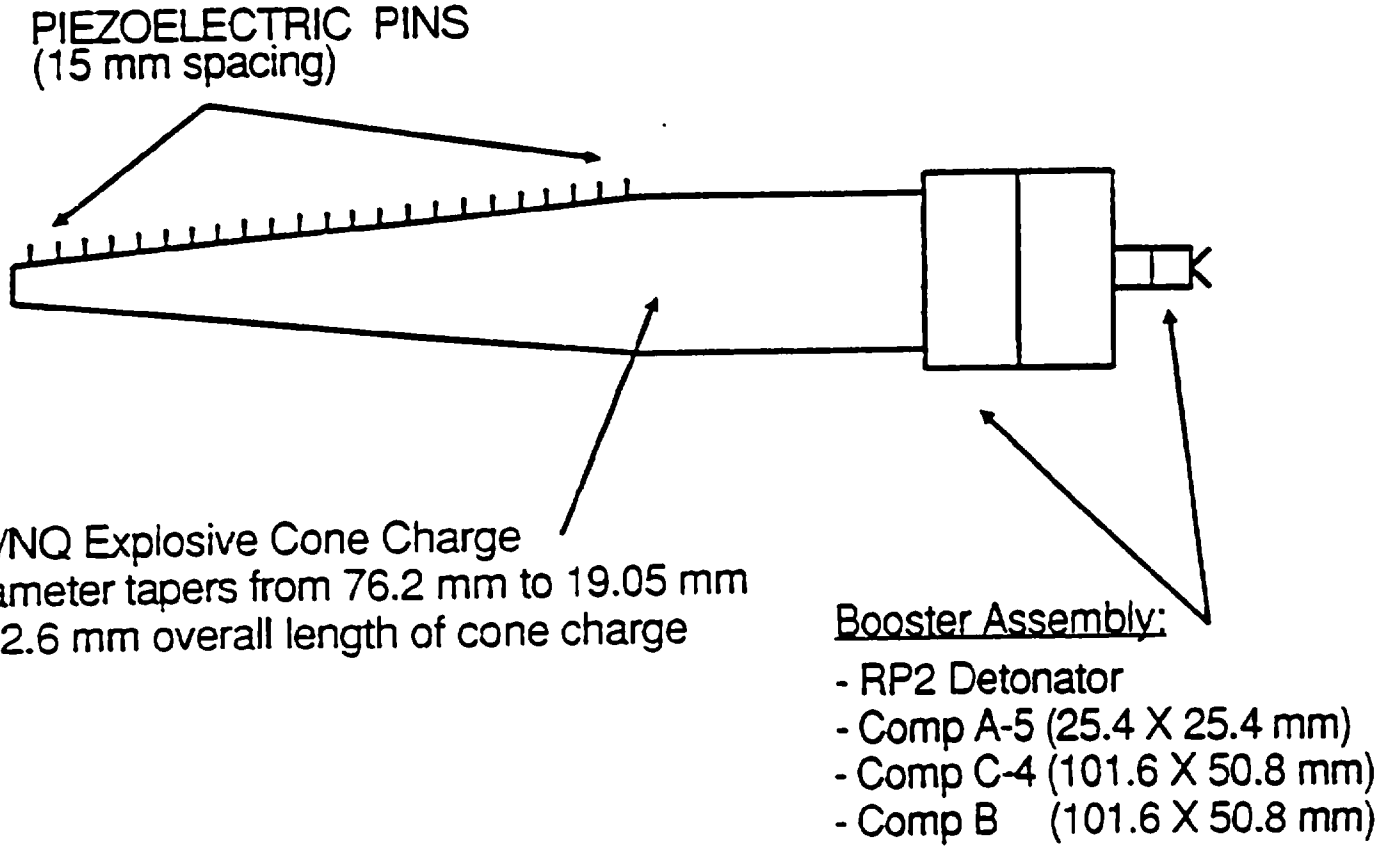

Figure 4. Schematic of a Conical Test Fixture for Measuring Critical Diameters of Explosives

cone technique have agreed within 6 mm of the values found by cylindrical configurations.

3. DETONATION VELOCITY/PRESSURE

Combination detonation velocity/pressure experiments were carried out using cast right circular cylinders of unconfined explosive. Cylinders were 203.2 mm in length and diameters varied from 19.0 to 50.8 mm. Three tests were carried out for each formulation at each of three diameters: 19.0; 25.4; and 50.8 mm for the TNT-based formulations and 25.4, 38.1 and 50.8 mm for the RDX-based formulations. Cylinders were instrumented with 11 piezoelectric pins spaced 15 mm apart and positioned vertically on two 152.4 by 152.4 mm square, 50.8 mm thick cold-rolled steel plates. Plate hardness varied between C9 and C10 on the Rockwell scale. Cylinders were boosted from the top with an assembly consisting of an RP2 detonator, a 25.4 mm long cylinder of Composition A-5 25.4 mm in diameter and a 50.8 mm long cylinder of Composition B donor that was 50.8 mm in diameter regardless of acceptor diameter. See Figure 5.

4. SHOCK SENSITIVITY

Shock sensitivity was determined using the modified expanded large scale gap test (ELSGT) (Reference 2). Explosives were cast into right circular steel tubes and machined flush with the ends. The tube was 279.4 mm long with an inside diameter of 73.15 mm and had a nominal wall thickness of 11.10 mm. Charges were instrumented with 10 piezoelectric pins spaced 25.4 mm apart along the length of the charge starting 25.4 mm from the top edge of the cylinder. The pins were inserted through the steel wall of the cylinder into preformed holes that protruded to the center of the explosive charge. The charge was centered vertically on top of a 19.05 mm thick 203.2 by 203.2 mm square steel (armor) plate which, in turn, rested on a plywood base. The booster assembly consisted of an RP2 detonator, a 25.4 mm thick cylinder of Composition A-5 25.4 mm in diameter, and a cylinder of Composition B 95.25 mm in diameter and 95.25 mm thick which acted as the donor.

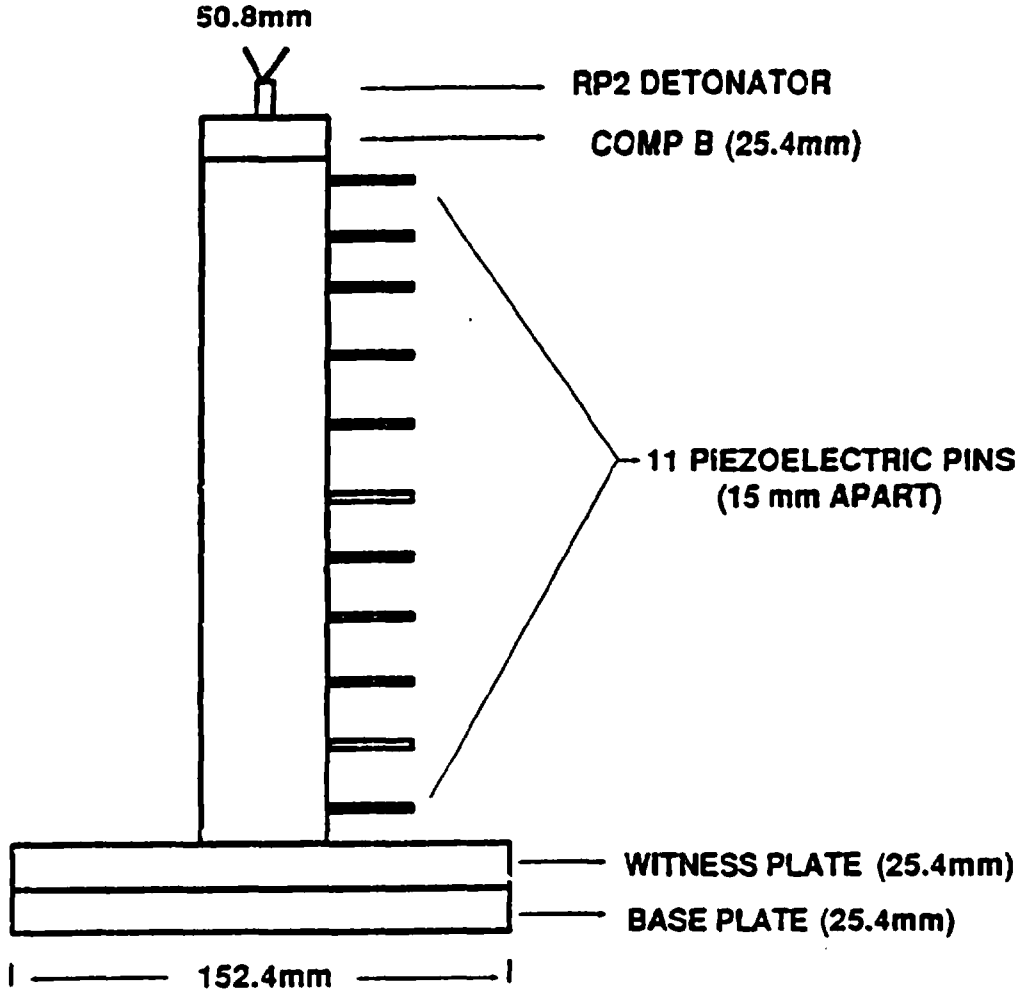

Figure 5. Schematic of a Test Fixture for Measuring Plate Dent and Detonation Velocities of Explosives

See Figure 6. Varying thicknesses of polymethyl methacrylate (PMMA) were placed between the booster assembly and the acceptor charges to vary the amount of transmitted shock. Tests were carried out using the Bruceton Up-Down method.

5. SLOW COOKOFF (Generic Hardware)

Slow cookoff tests were carried out in steel pipe nipples with end caps. The pipes were 152.4 mm long schedule 80 steel with an inside diameter of 101.6 mm and a nominal wall thickness of 6.02 mm. See Figure 7. After one end cap was placed onto the nipple and tightened, the device was then lined with a thin coating of R45HT polybutadiene-based polymer. The polymer was applied to the entire inner metal surface of the container and then the container was inverted to allow excess polymer to drain during the curing process. The explosive formulation was cast into the lined hardware to 12.7 mm below the open end. The remainder was filled with Tuff Seal^{R} to a level flush with the open end. This rubbery material was used to prevent the explosive from shifting during transport and also to prevent it from coming into contact with the bare metal of the end cap during the test. The remaining end cap was tightened onto the open end. Free volume consisted of a small space between the upper Tuff Seal^{R} level and the inner surface of the upper end cap and shrinkage void, if any, in the explosive not filled with Tuff Seal^{R}. The closed loop cookoff system consisted of a heater oven, an inner hardware oven, and a blower (See Reference 3 for details). The test hardware was placed in the hardware oven in the horizontal position. Tests were conducted three at a time and in triplicate for each formulation. Test items were heated to a temperature 55^{o}C below the predicted reaction temperature, allowed to stabilize for 1 hour, then heated at a rate of 3.3^{o}C per hour. Predicted reaction temperatures were calculated from DSC data (Reference 1) whereby the least squares fit of the data was extrapolated to the above heating rate. No consideration was given to the wall thickness of the test hardware. Thermocouples were placed at strategic positions within

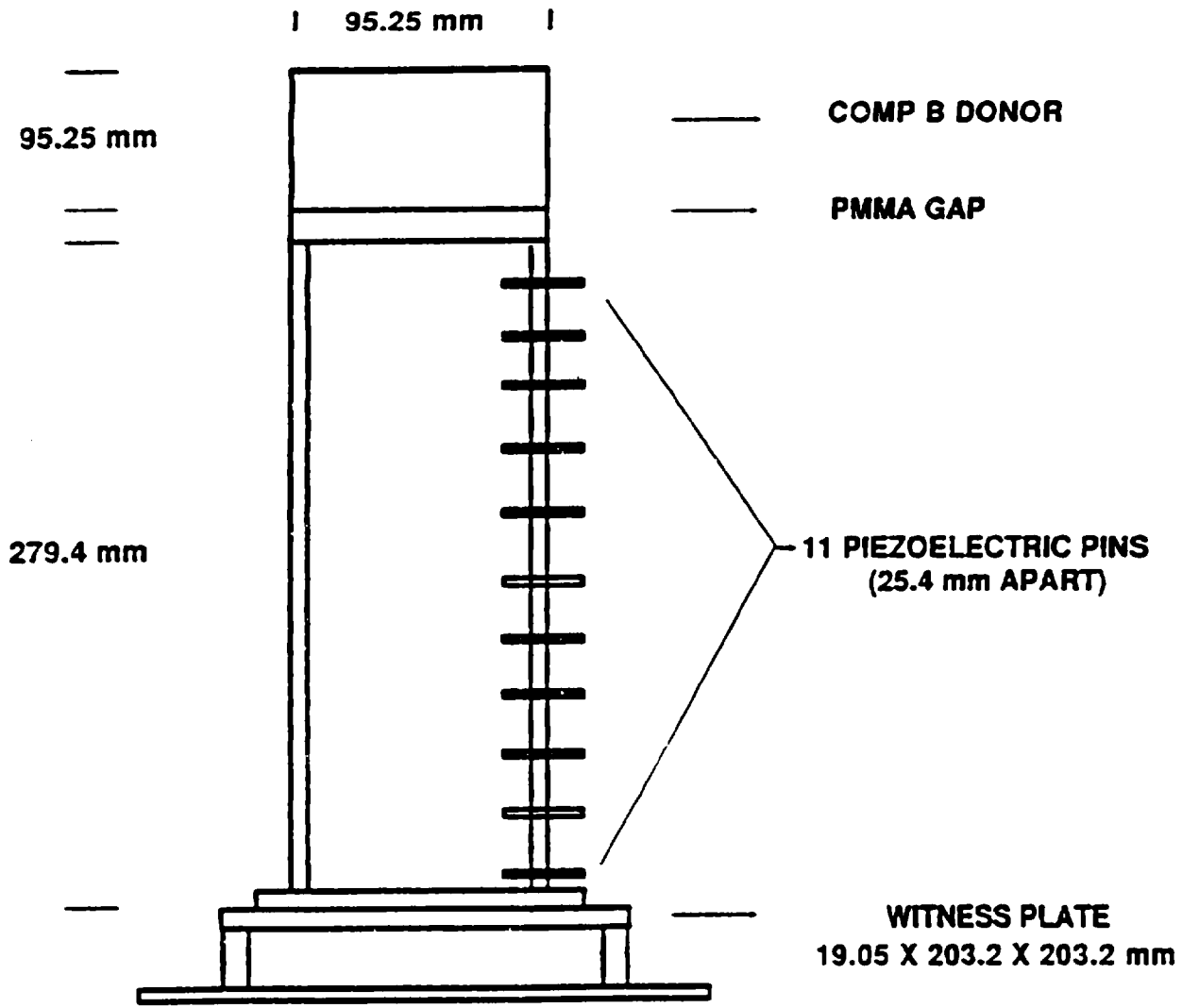

Figure 6. Schematic of Modified ELSGT Configuration

HARDWARE:

- 152.4 mm long schedule 80 steel pipe with end caps
- 101.6 mm inside diameter
- 6.02 mm nominal wall thickness
- lined with R45HT polymer
- cast explosive topped with Tuff Seal

TEST PROCEDURE:

- items were heated to 55 degrees C below the predicted reaction temperature
- temperature held constant for 1 hour
- items then heated at a rate of 3.3 degrees C per hour

Figure 7. Schematic of Slow Cookoff Test Apparatus Using Generic Hardware

the closed loop system and on the outer surface of the test hardware (Reference 3).

6. SLOW COOKOFF (SCO Units)

Slow cookoff tests were carried out in small-scale cookoff bomb (SCB) units as generally described below and in Reference 4. The bomb body was constructed from mild steel (1026) tubing with the bottom end plate welded into position. The inside diameter was 63.5 mm, the wall thickness 6.35 mm, and the inside depth 127 mm. The inside walls of the bomb body were lined with asphalt. The explosive charges were cast into cylinders with a pre-formed hole down the centerline to accommodate a type K thermocouple. The charges were machined to 57.15 mm in diameter and 107.95 mm in length and were inserted into the bomb body. After the end cap was placed onto the bomb body and tightened, the thermocouple was inserted into the explosive and sealed into the end cap with a special Swagelok fitting. The SCB unit was sandwiched between two witness plates, 127 by 127 by 12.7 mm, constructed from 1018 mild steel and secured by 4 bolts. The SCB unit was placed in a specially designed oven, heated to 105°C, held for six hours and then heated at a rate of 3.3°C/hour until reaction. A new oven was used for each test. See Figure 8.

7. BULLET IMPACT

Bullet impact tests were carried out with schedule 80 pipe 152.4 mm ID by 304.8 mm in length with end caps, filled with the explosive formulation. Three .50-caliber, single-shot Mann barrels were used for these tests. The weapons were placed side by side and sequenced 100 milliseconds apart to simulate a three-round burst from a .50-caliber machine gun. Two 16 mm high-speed motion-picture cameras, operated at 4,000 frames per second, and two CCTV cameras were used to record the tests. Velocity screens were used to determine the average impact velocity for the .50-caliber ammunition lot. The instrumentation and experimental arrangements are described in Reference 3.

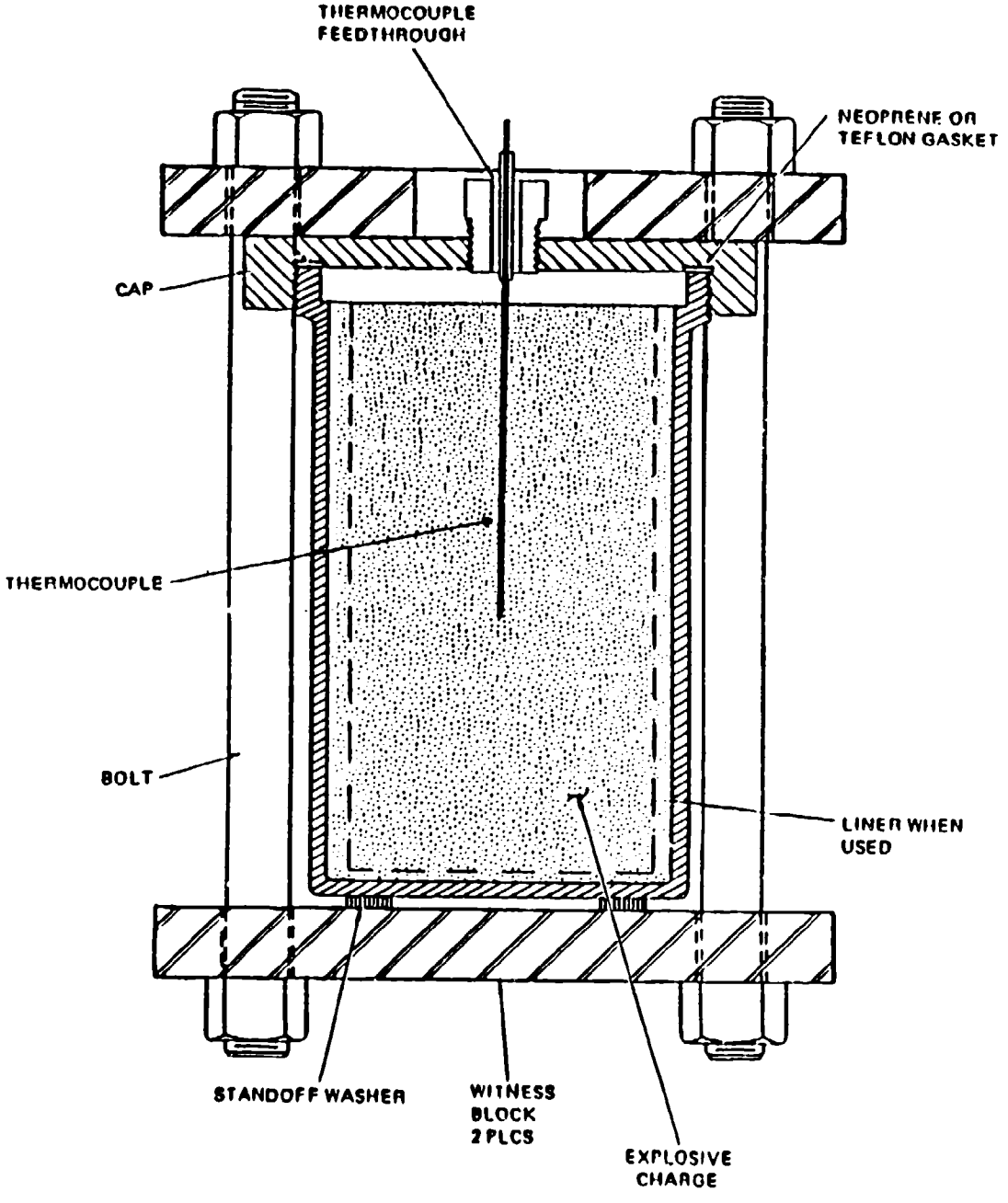

Figure 8. Schematic of a Small-Scale Cookoff Bomb (SCB) Unit

8. DENSITY

Particle densities were obtained with a Penta-Pycnometer, Model PP-4, manufactured by Quantachrome Corporation. Nitrogen was used as the displacing fluid. Sample mass for both HBCNQ and SNQ was around 6 grams and around 1 gram for needle-like NQ. Bulk (packing) densities for HBCNQ and SNQ were obtained by the tapping method where a volumetric container was tapped until a constant volume of sample was maintained.

SECTION III

RESULTS

1. DIFFERENTIAL SCANNING CALORIMETRY (DSC)

Typical DSC thermograms, scan rates of 10°C per minute, for HBCNQ (297-420 u), HBCNQ (105-210 u), SNQ (297-420 u), SNQ (105-210 u), TNT, TNT/HBCNQ (297-420 u), TNT/HBCNQ (105-210 u), TNT/SNQ (297-420 u), and TNT/SNQ (105-210 u) are shown in Figures 9, 10, 11, 12, 13, 14, 15, 16 and 17, respectively. HBCNQ thermograms are characterized by a broad, low intensity exotherm prior to the main exotherm, while those from SNQ show a sharp exotherm preceded by a small endotherm. In all cases, the main exotherm associated with HBCNQ occurs around 20°C before that of SNQ. A thermogram (not shown) from the needle-like NQ is similar in appearance to that from SNQ. The peak temperature associated with its single exotherm peak occurs only about 4°C lower than that associated with SNQ suggesting similar decomposition characteristics. The exotherms associated with the TNT-based formulations are characterized by two exothermic areas. The lower temperature area is assumed to be associated with NQ decomposition and the latter with TNT decomposition. Furthermore, the exothermic area associated with HBCNQ in the TNT formulations is characterized generally by two intense peaks at low heating rates, while the same area associated with SNQ is typified by only a single peak.

Typical DSC thermograms, scan rate of 10°C/minute, for RDX/HBCNQ and RDX/SNQ are shown in Figures 18 and 19, respectively. NQ particle size range for the RDX-based formulations is 210-297 microns. The thermograms for the former are characterized by broad, multiplets at lower scan rates, while those for the latter consist of relatively sharp singlets for all scan rates. Exotherm peak temperature associated with the RDX/HBCNQ formulation occurs about 10°C lower than the corresponding peak for the RDX/SNQ formulation. Apparent activation energies for the decomposition process for both types of NQ and the various formulations are shown in Table 1.

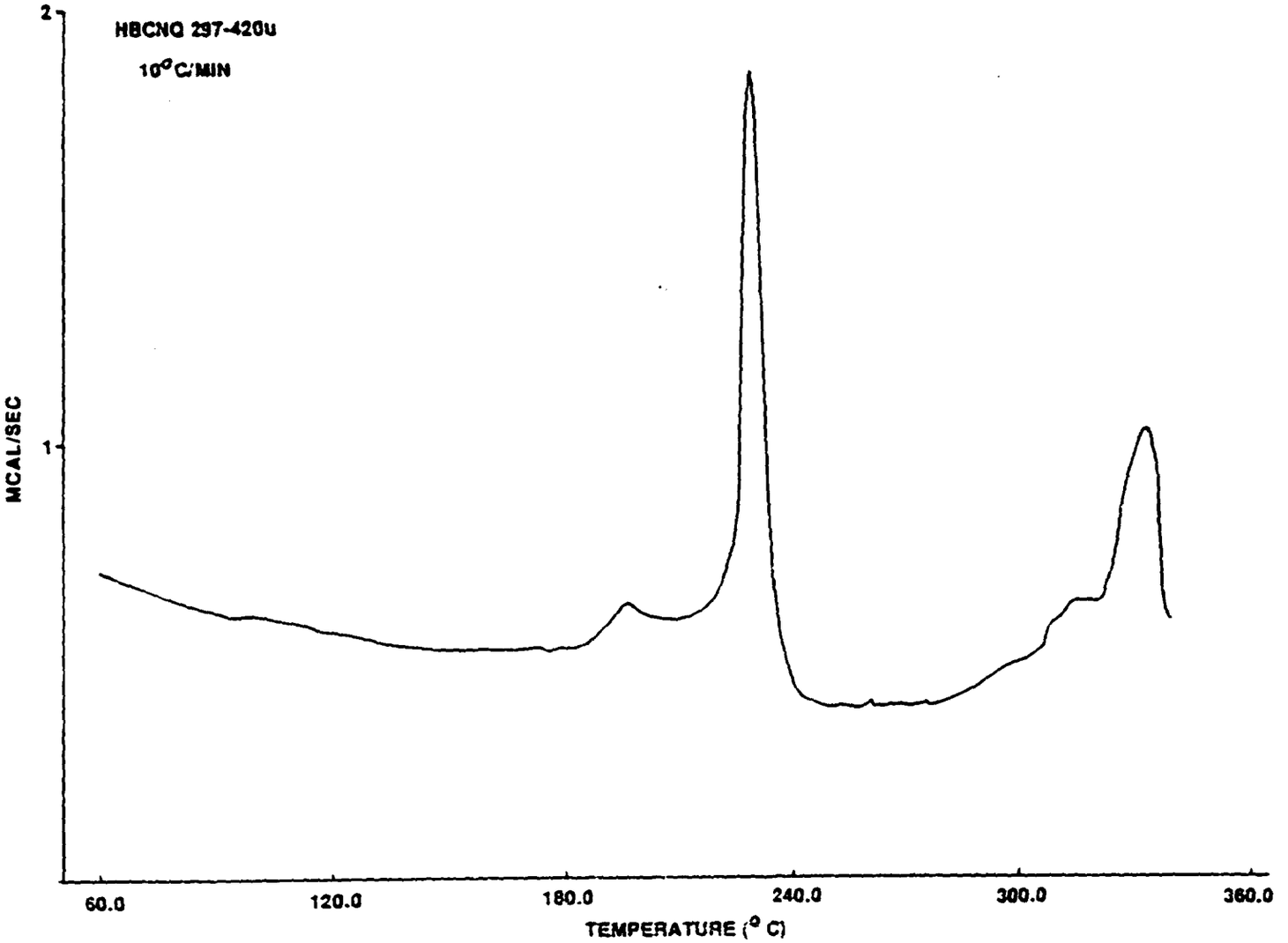

Figure 9. DSC Thermogram of HBCNQ (297-420 u)

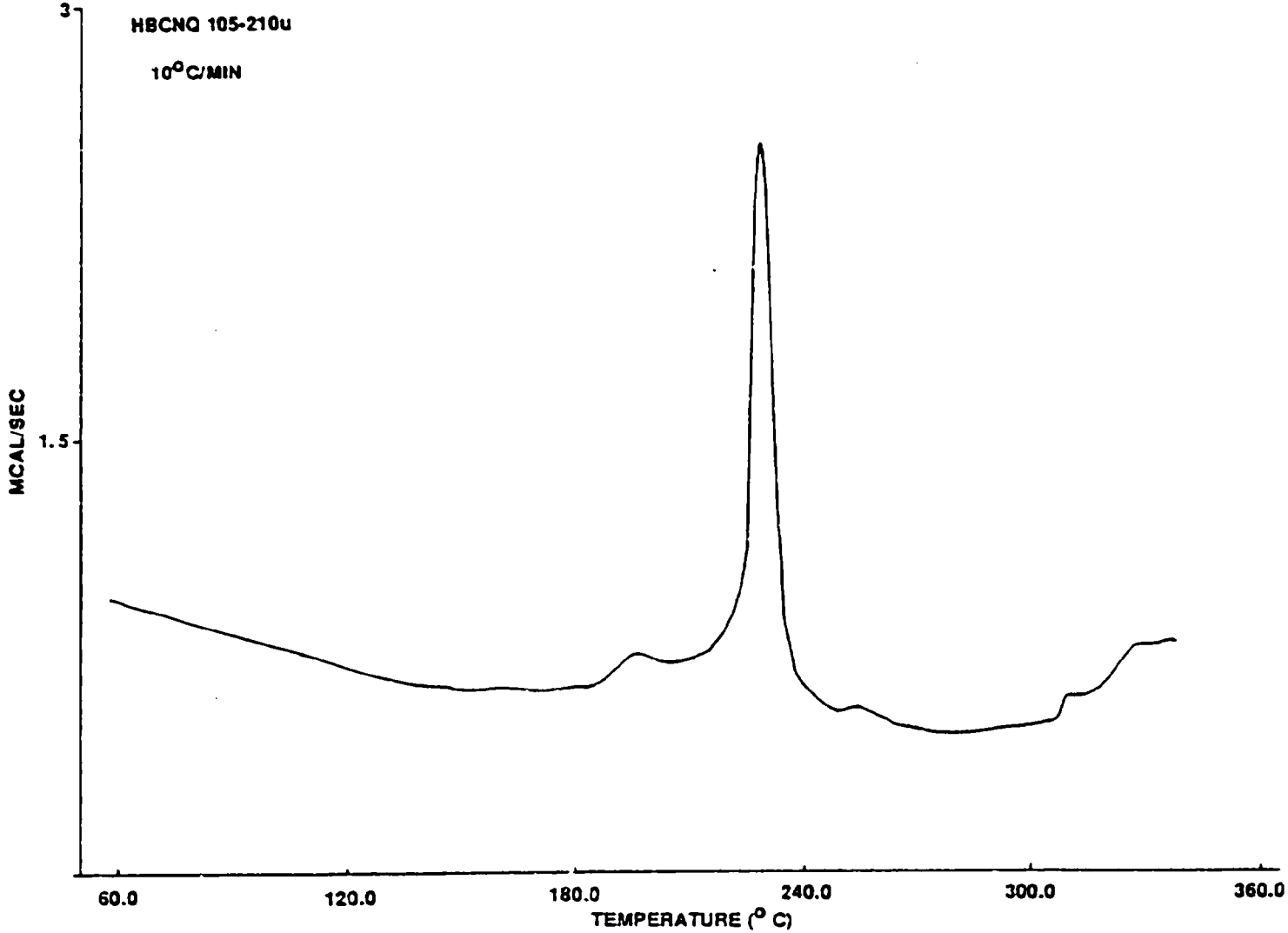

Figure 10. DSC Thermogram of HBCNQ (105-210 u)

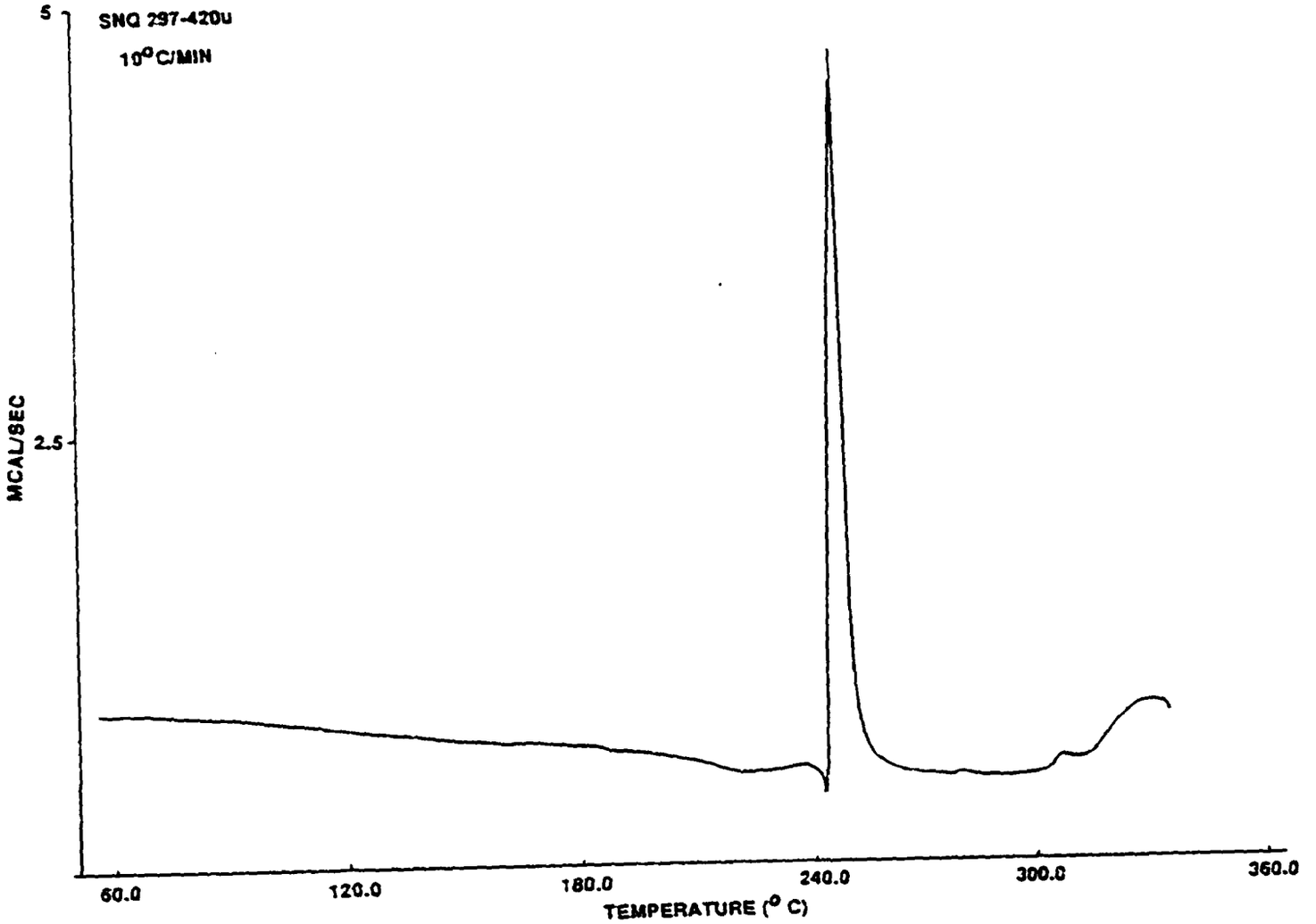

Figure 11. DSC Thermogram of SNQ (297-420 u)

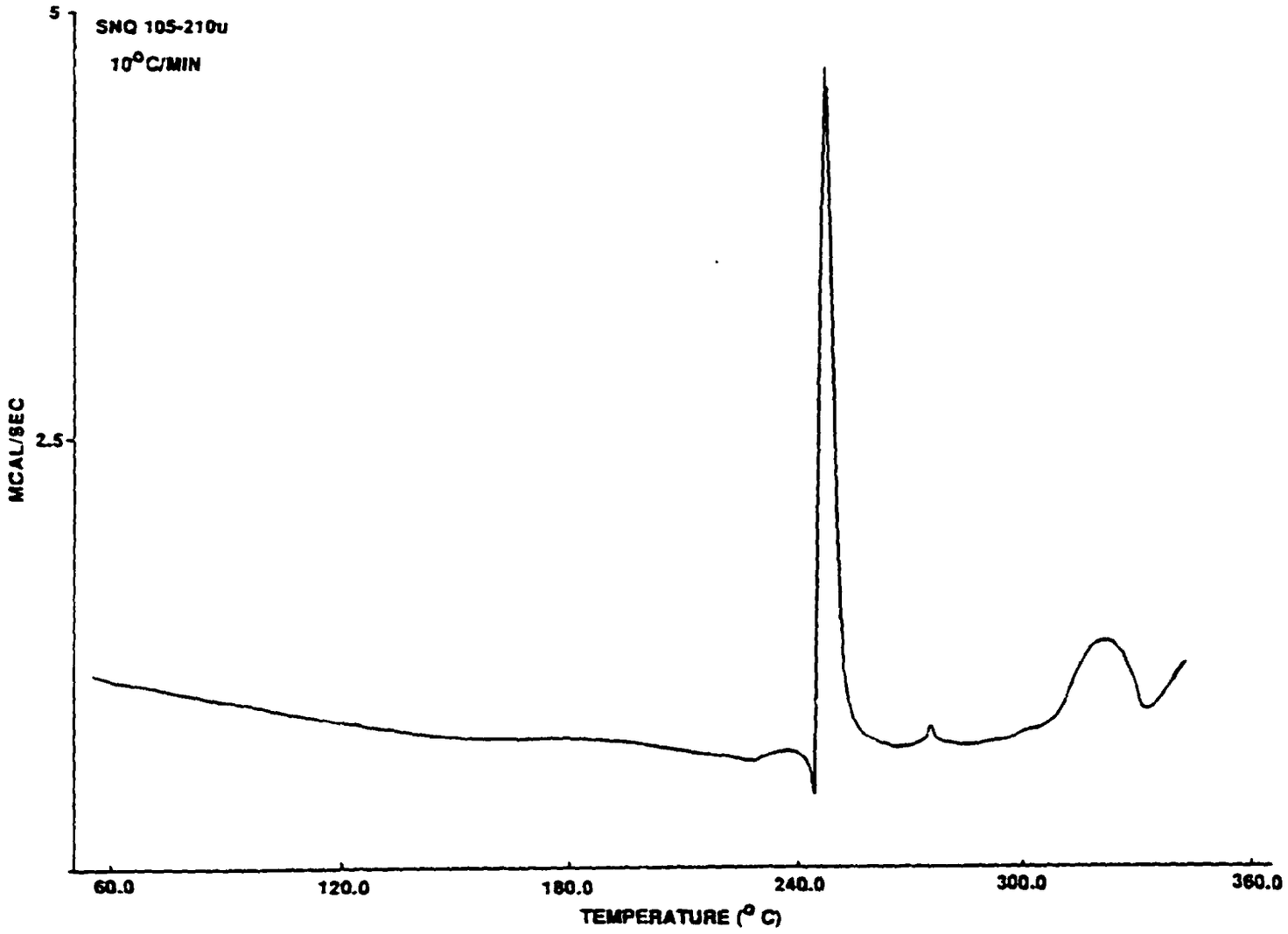

Figure 12. DSC Thermogram of SNQ (105-210 u)

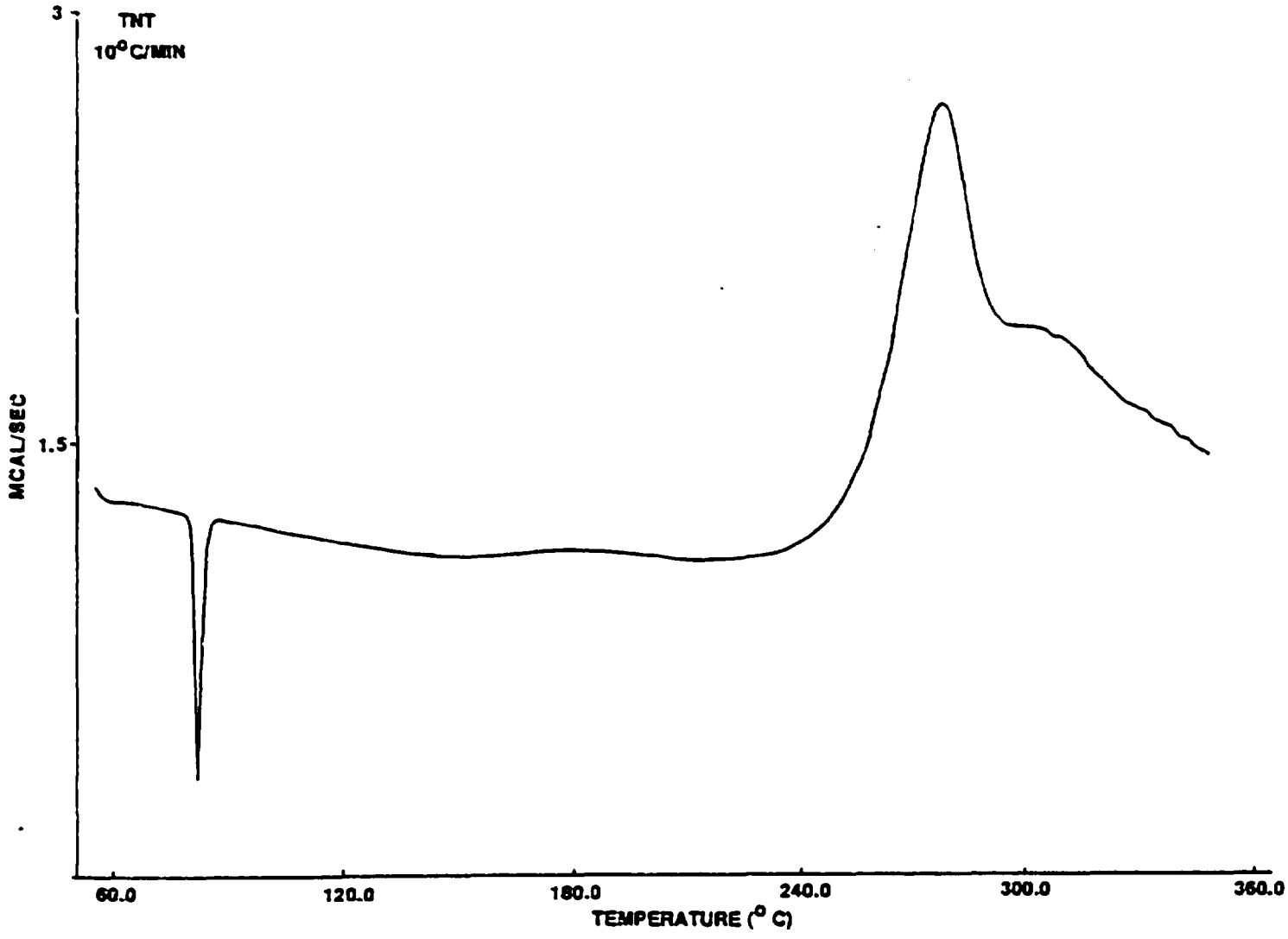

Figure 13. DSC Thermogram of TNT

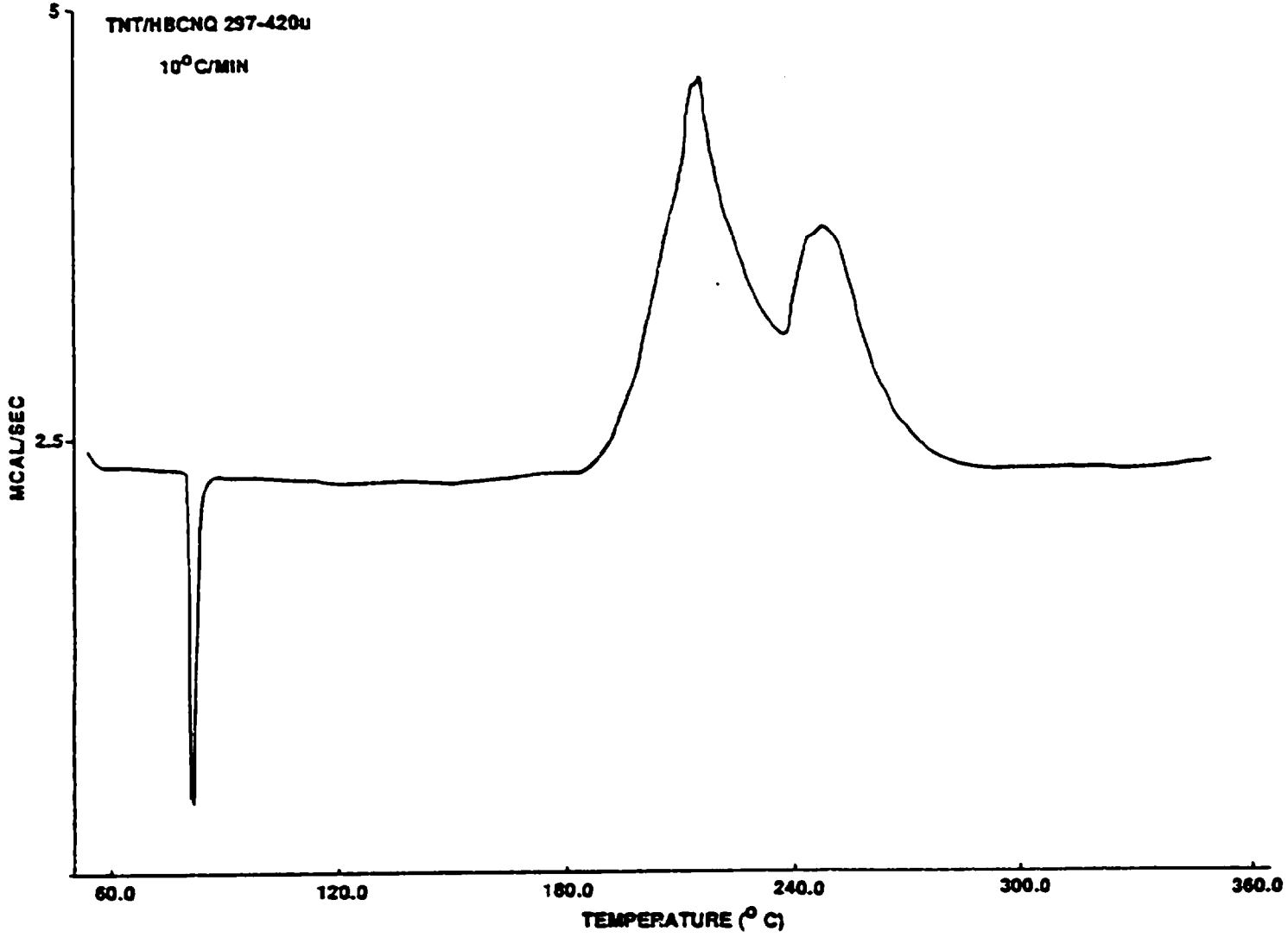

Figure 14. DSC Thermogram of TNT/HBCNQ (297-420 u)

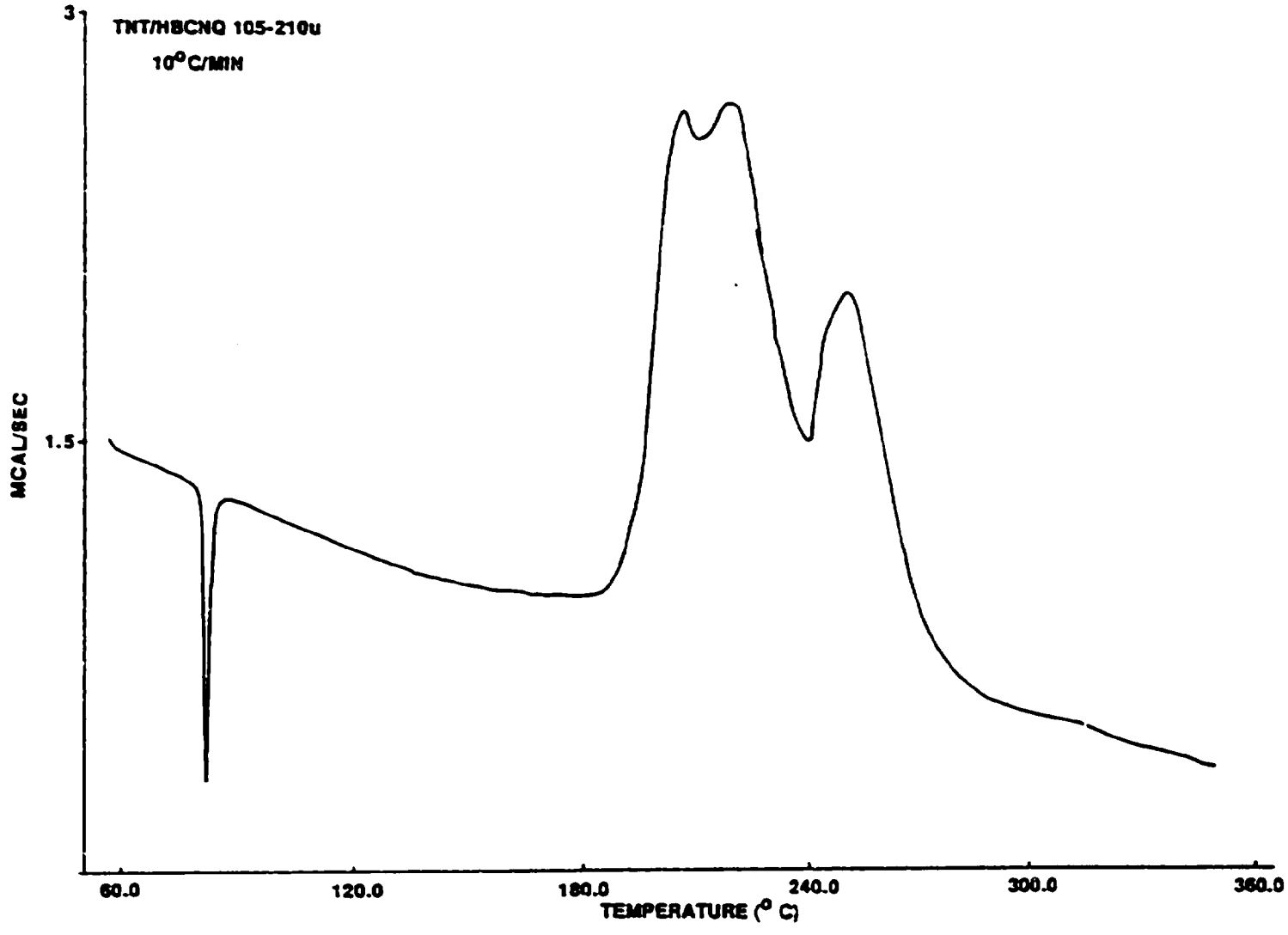

Figure 15. DSC Thermogram of TNT/HBCNQ (105-210 u)

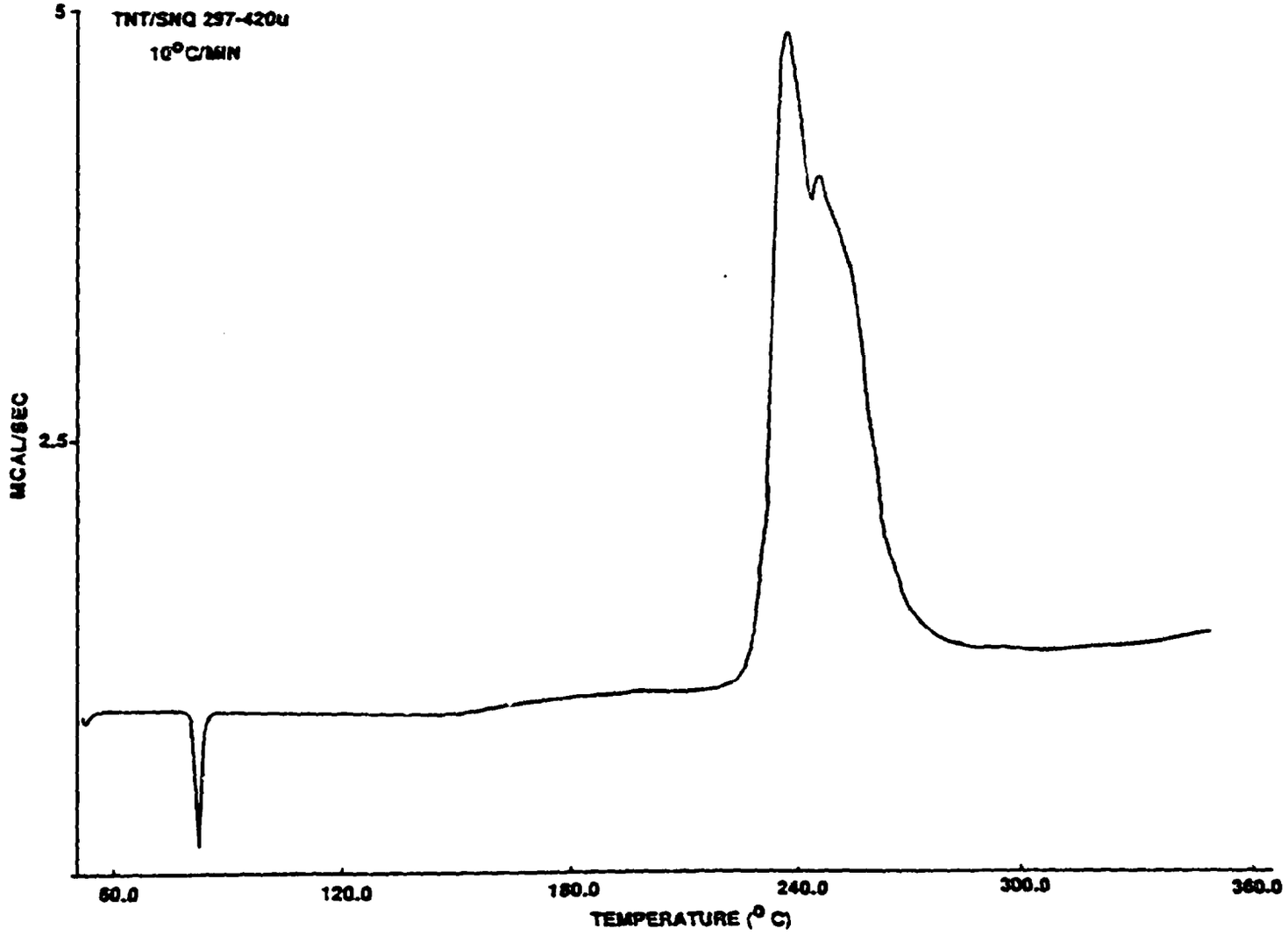

Figure 16. DSC Thermogram of TNT/SNQ (297-420 u)

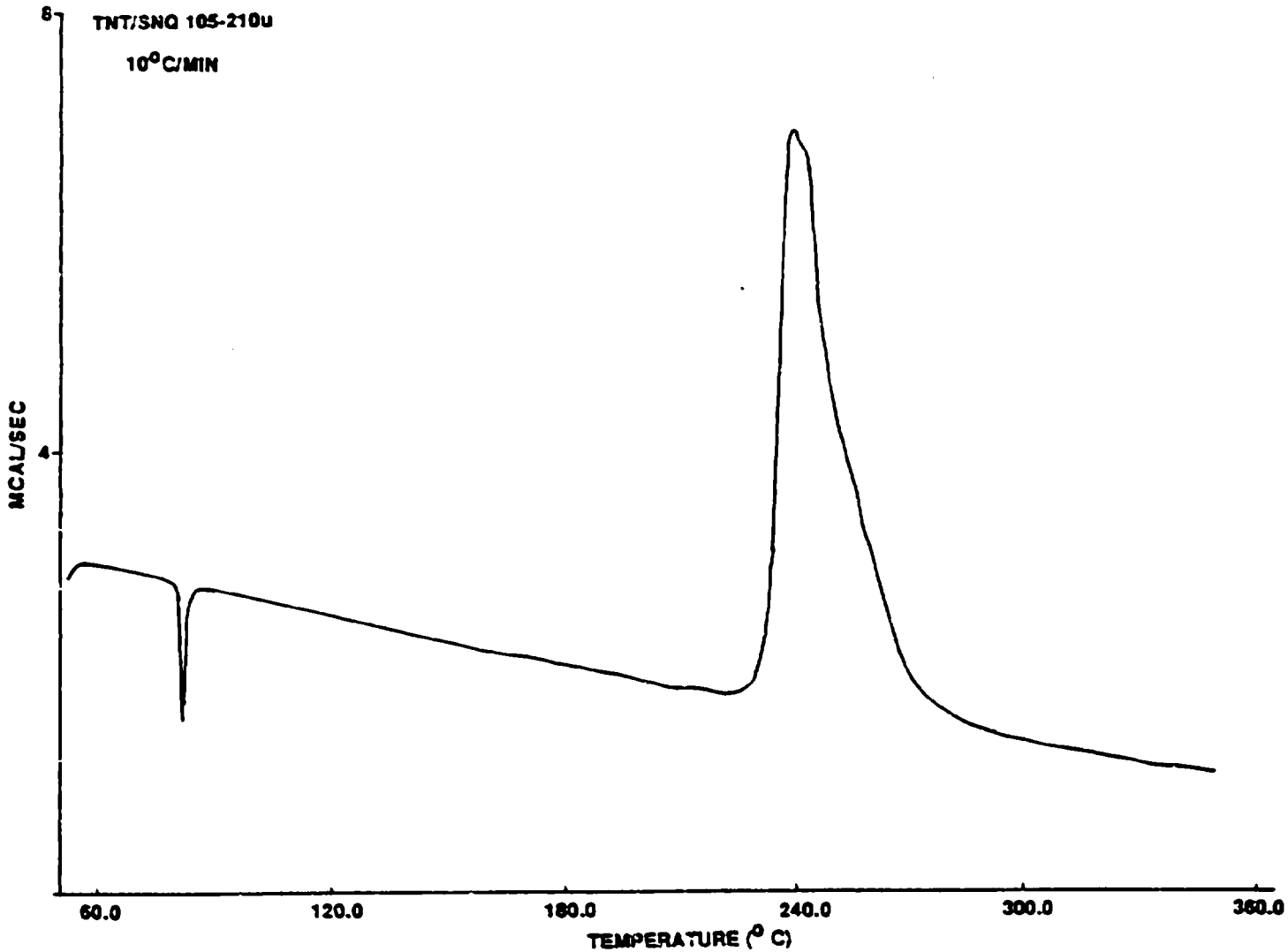

Figure 17. DSC Tnermogram of TNT/SNQ (105-210 u)

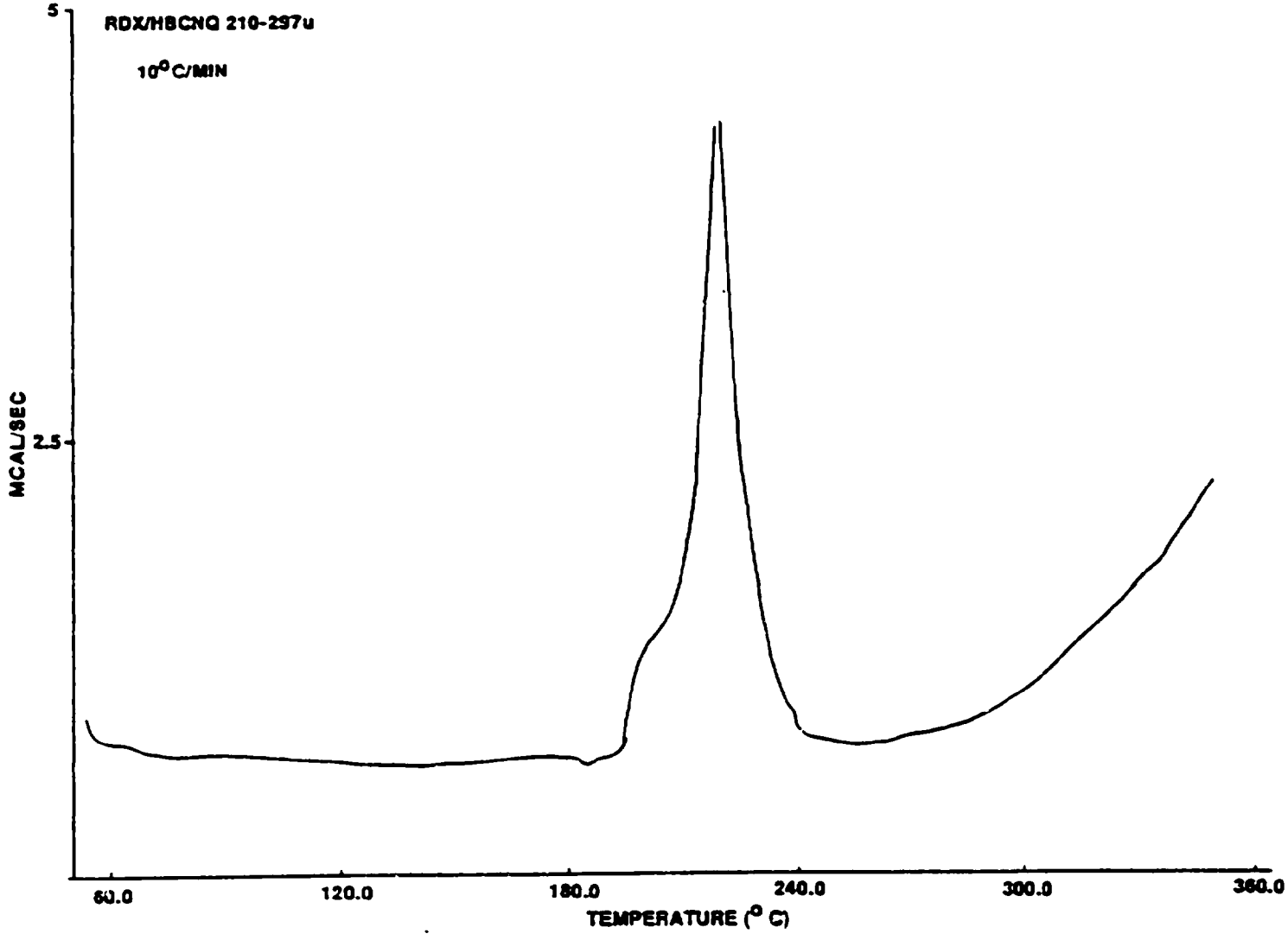

Figure 18. DSC Thermogram of RDX/HBCNQ (210-297 u)

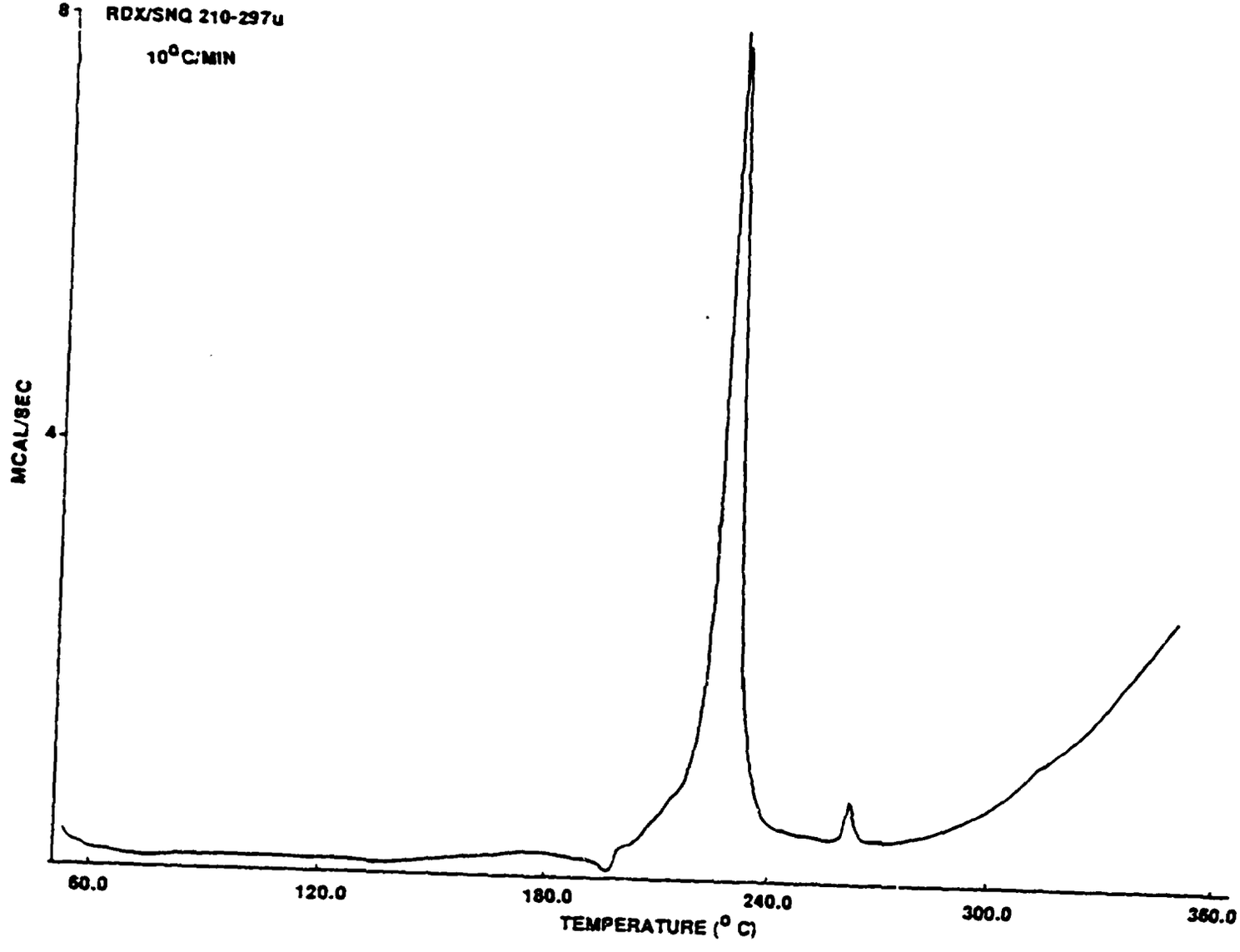

Figure 19. DSC Thermogram of RDX/SNQ (210-297 u)

TABLE 1. ACTIVATION ENERGIES FOR HBCNQ, SNQ, AND THE TNT- AND RDX-BASED FORMULATIONS

Compound/Formulation	Particle Size (microns)	Activation Energy (Kcal/mole)
HBCNQ	297-420	29.6 ± 0.9
HBCNQ	105-210	29.3 ± 0.7
SNQ	297-420	38.1 ± 0.9
SNQ	105-210	35.9 ± 0.6
SNQ	crushed	36.4 ± 0.4
TNT/HBCNQ	297-420	27.8 ± 1.7
TNT/HBCNQ	105-210	24.7 ± 1.7
TNT/SNQ	297-420	31.6 ± 1.5
TNT/SNQ	105-210	31.6 ± 0.7
RDX/HBCNQ	210-297	28.5 ± 0.6
RDX/SNQ	210-297	33.4 ± 0.7

2. CRITICAL DIAMETER

The critical diameters for the formulations TNT/HBCNQ (297-420 u), TNT/SNQ (297-420 u), RDX/HBCNQ (210-297 u), TNT/HBCNQ (105-210 u) and TNT/SNQ (105-210 u) are 29 $\pm$ 3, 25 $\pm$ 3, 24 $\pm$ 3, <19 and <19 mm, respectively. The graphical representations of the measured detonation velocities versus reciprocal radius for each of the above experiments are shown in Figures 20, 21, 22, 23, and 24. The data gleaned from these experiments are summarized in Table 2. Also included in the table are the calculated charge detonation velocities, D, at a diameter of 50.8 mm and the percent of the ideal detonation velocity of pure NQ, Di(NQ), at the given density. The detonation velocity of the NQ component of the mixture and Di(NQ) value can be calculated from the known ideal curves and the simple additivity principle (References 5 and 6). Critical diameters were determined from pin data. The critical diameter for the RDX/SNQ formulation was not determined.

3. DETONATION VELOCITY/PRESSURE

The detonation velocities for the TNT-based formulations have been obtained at charge diameters of 50.8, 25.4, and 19.05 mm and for the RDX-based formulation at 50.8, 38.1, and 25.4 mm. Detonation pressures based on plate dent measurements were obtained only for the 50.8 mm-diameter charges. These data, along with the corresponding calculated D(NQ) values are shown in Table 3.

4. SHOCK SENSITIVITY

a. TNT-NQ Series (297-420 micron NQ)

The results from the modified ELSGT series for the TNT/NQ (297-420 micron) melt cast system are summarized in Table 4 and run to detonation curves are shown in Figures 25 and 26. HBCNQ yields a 50 percent gap thickness between 80.96 (Go) and 82.55 mm (No Go) of PMMA based on standard witness plate damage data. These thicknesses correspond to 37.3 and 35.9 kbar of input pressure, respectively. The 50 percent gap thickness for SNQ

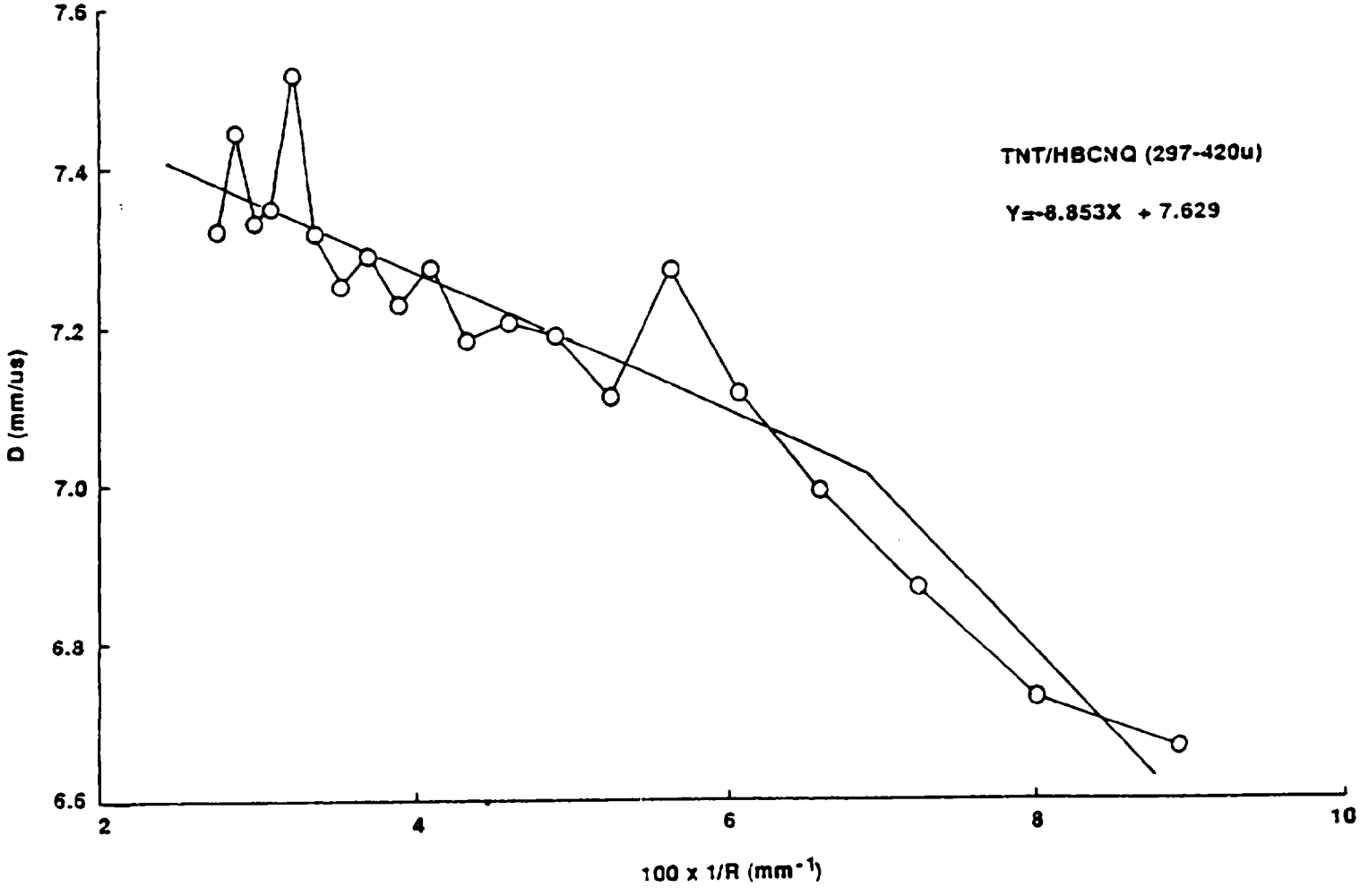

Figure 20. Critical Diameter Pin Data for TNT/HBCNQ (297-420 u)

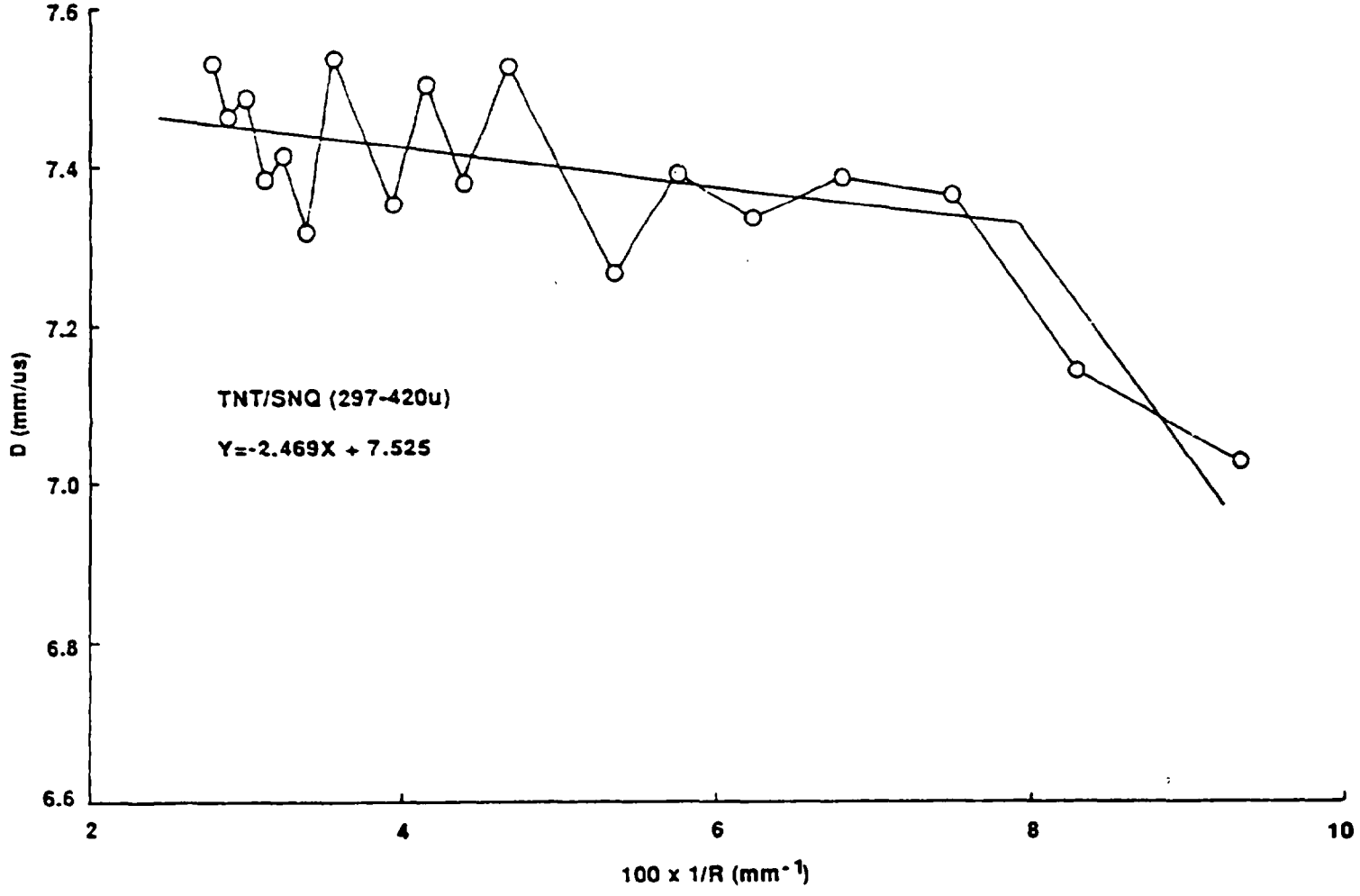

Figure 21. Critical Diameter Pin Data for TNT/SNQ (297-420 u)

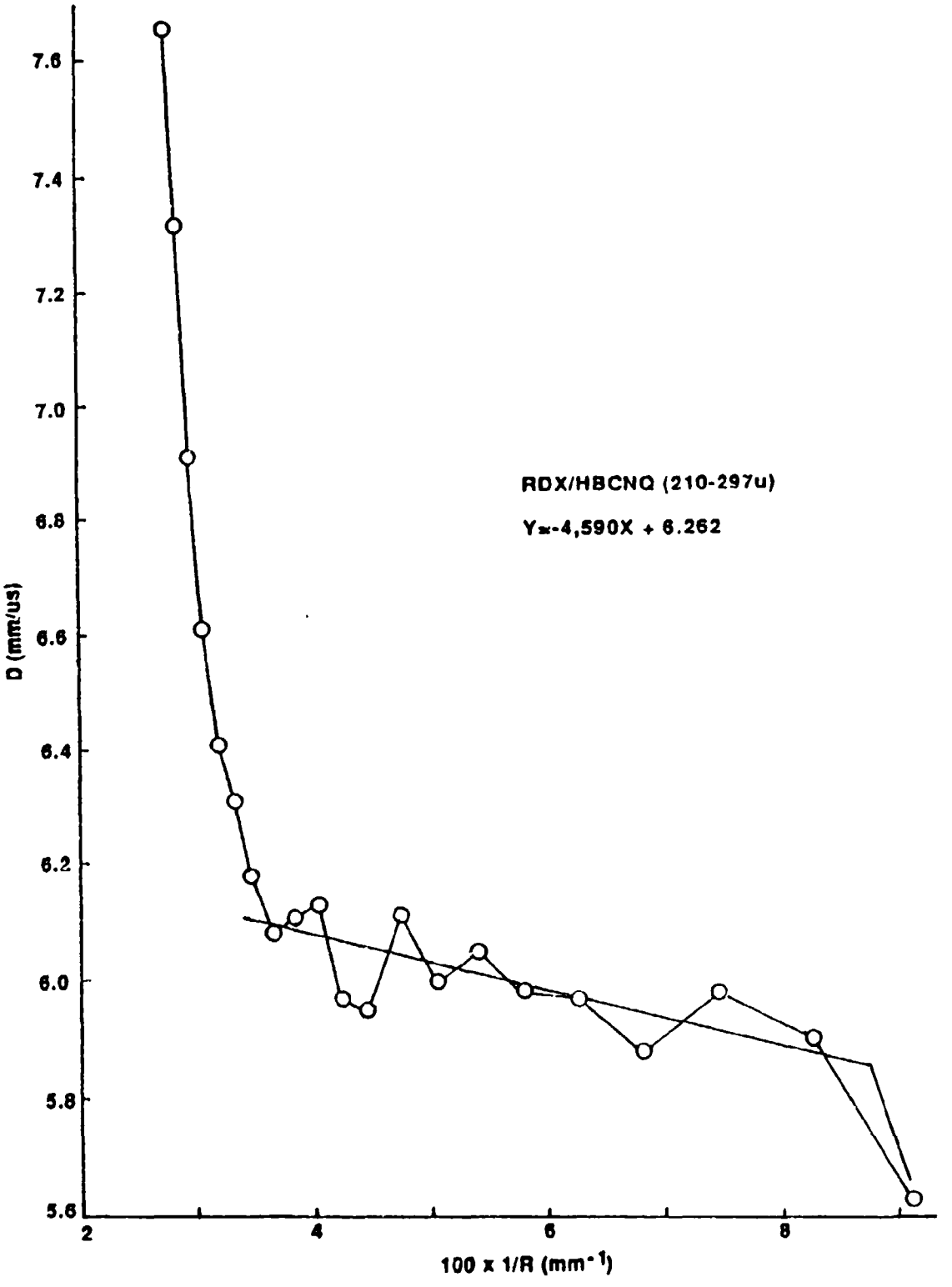

Figure 22. Critical Diameter Pin Data for RDX/HBCNQ (210-297 u)

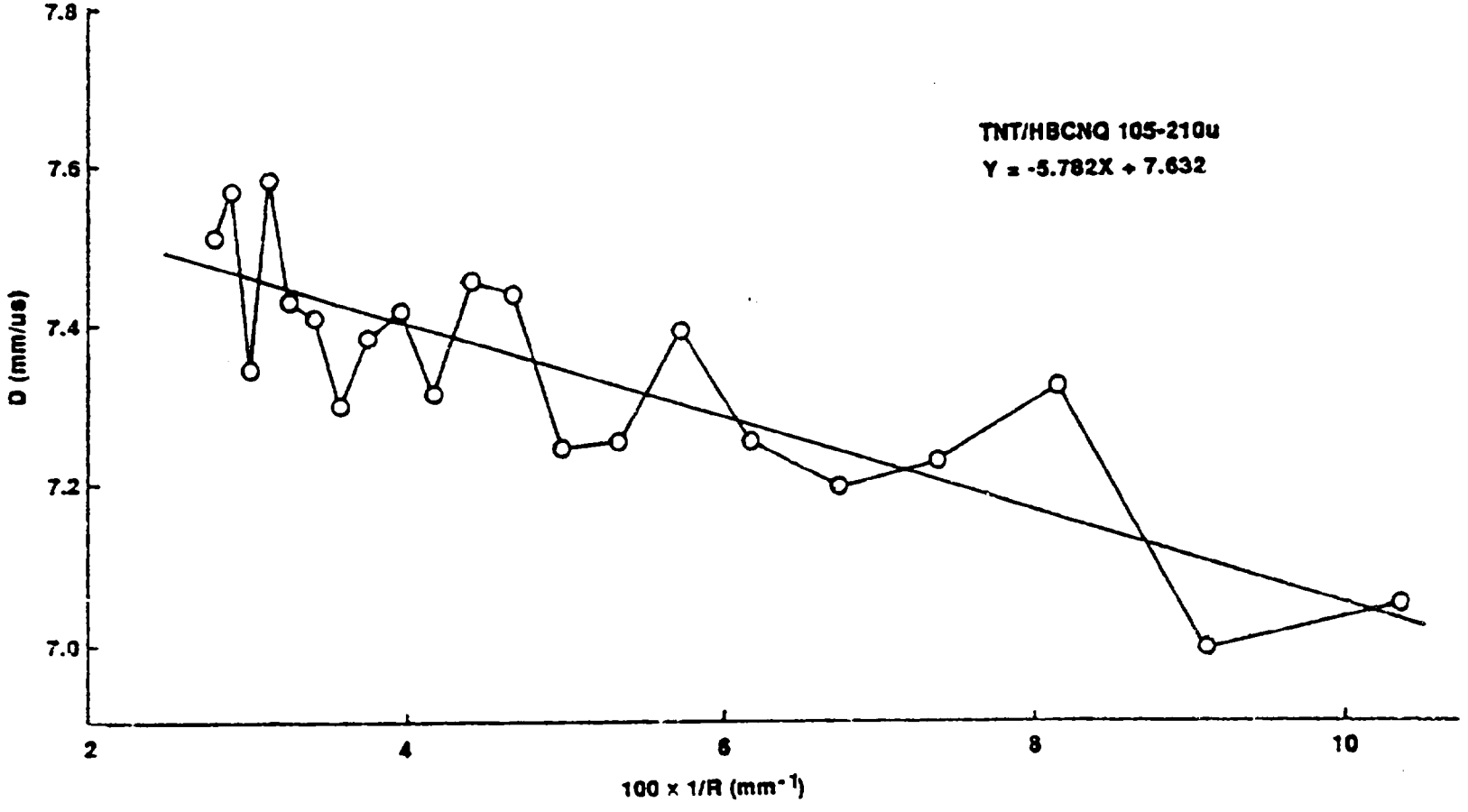

Figure 23. Critical Diameter Pin Data for TNT/HBCNQ (105-210 u)

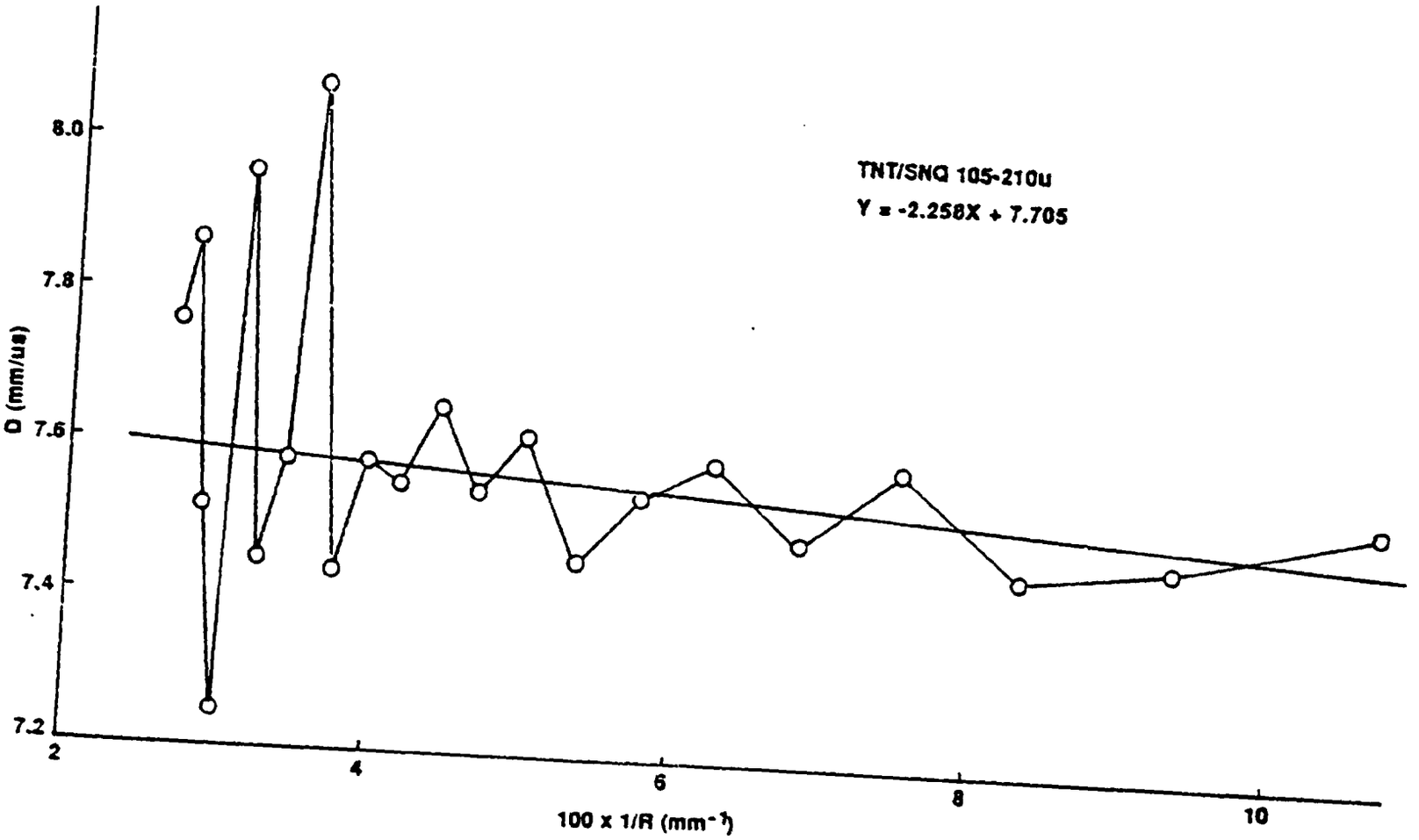

Figure 24. Critical Diameter Pin Data for TNT/SNQ (105-210 u)

TABLE 2. CRITICAL DIAMETER AND DETONATION VELOCITIES FOR TNT- AND RDX-BASED NQ FORMULATIONS

Formulation	Particle Size (u)	Critical Diameter (mm)	Density (g/cm^3)	Calc'd D at[1] 50.8mm (mm/us)	%Di(NQ)[2]
TNT/HBCNQ	105-210	<19	1.663	7.40	93
TNT/HBCNQ	297-420	29 ± 3	1.643	7.28	92
TNT/SNQ	105-210	<19	1.638	7.62	101
TNT/SNQ	297-420	25 ± 3	1.636	7.43	99
RDX/HBCNQ	210-297	24 ± 3	1.60	6.08	66

1. Calculated detonation velocities at a diameter of 50.8 mm from regression analysis equations shown in Figures 20, 21, 22, 23, and 24.

2. The detonation velocity of the NQ component of the charge, D(NQ), and the ideal detonation velocity of pure NQ at the given density, D_i(NQ), are calculated from the ideal equations and the additivity principle (Reference 5).

Table 3. DETONATION VELOCITY/PRESSURE TEST DATA SUMMARY
(295 Kbars Input Pressure)

Formulation	Particle Size (microns)	Diameter (mm)	Dv[1] (mm/us)	Density (g/cm^3)	D(NQ)[2] (mm/us)	P[3] (Kbars)
TNT/HBCNQ	105-210	50.8	7.197	1.622	7.46	205
			7.082	1.624	7.23	208
			7.107	1.626	7.28	215
TNT/HBCNQ	297-420	50.8	7.030	1.634	7.11	209
			6.993	1.638	7.15	211
			6.979	1.638	7.15	208
TNT/SNQ	105-210	50.8	7.273	1.632	7.61	208
			7.287	1.633	7.63	212
			7.231	1.625	7.53	212
		25.4	7.099	1.646	7.17	
			7.109	1.647	7.18	
			7.108	1.624	7.29	
		19.05	6.962	1.639	7.14	
			6.967	1.644	7.16	
TNT/SNQ	297-420	50.8	7.070	1.635	7.19	216
			7.192	1.636	7.43	219
			7.293	1.640	7.15	218
		25.4	6.976	1.647	7.17	
			6.669	1.645	7.17	
			6.715	1.658	7.21	
		19.05	6.775	1.626	6.62	
RDX/HBCNQ	210-297	50.8	6.058	1.629	5.07	67
			5.949	1.635	4.90	65
			5.931	1.643	4.86	65
		38.1	5.912	1.640	4.84	
			5.684	1.619	4.54	
			5.650	1.612	4.50	
			5.644	1.600	4.51	
			5.564	1.612	4.37	
		25.4	5.677	1.631	4.51	
			5.617	1.627	4.43	
RDX/SNQ	210-297	50.8	6.827	1.618	6.21	112
			7.267	1.619	6.85	137
			7.017	1.612	6.49	139
		38.1	6.000	1.631	4.98	
			5.629	1.600	4.49	
			5.562	1.580	4.42	
			5.566	1.590	4.41	
		25.4	5.857	1.622	4.78	
			5.795	1.644	4.66	
			5.841	1.627	4.75	

1. Measured detonation velocity
2. Calculated NQ detonation velocity
3. Detonation pressure from plate dent experiments

TABLE 4. MODIFIED ELSGT RESULTS FOR TNT/NQ MELT CAST SYSTEMS (297-420 micron NQ)

Type NQ	Density (gm/cm³)	% TMD[1]	PMMA Thickness (mm)	Velocity (mm/us)	Comments
HBCNQ	1.640	95.8	101.6	No Go	Witness Plate deformed about 38 mm Case split into two pieces
	1.635	95.5	88.90	No Go	Witness plate deformed about 51 mm Case fragmented into large pieces
	1.638	95.7	82.55	No Go[2]	Witness Plate deformed Case fragmented into medium-to-large pieces
	1.631	95.3	80.96	Go[3]	Witness Plate holed and cracked Case fragmented into small pieces
	1.689	98.7	79.38	Go[4]	Witness Plate holed, cracked and deformed Case fragmented into small pieces
	1.647	96.2	76.20	Go[4]	Witness plate holed, cracked and deformed Case fragmented into small, highly sheared pieces
	1.646	96.1	25.40	7.20 ± 0.09[5]	Witness plate holed Case fragmented into small pieces
SNQ	1.585	92.6	101.6	No Go	Witness plate slightly deformed Case broken into two pieces
	1.593	93.0	88.90	No Go	Witness plate deformed Case fragmented into large & small pieces
	1.638	95.7	87.31	No Go[2]	Witness plate deformed about 76 mm Case fragmented into medium-to-large pieces
	1.639	95.7	85.72	2.67-4.23[6]	Witness plate holed and broken into 3 pieces Case fragmented into small pieces
	1.618	94.5	82.55	7.13 ± 0.12[7]	Witness plate holed and broken in half Case fragmented into small pieces
	1.585	92.6	76.20	7.11 ± 0.10[8]	Witness plate holed and broken in half Case fragmented into small, very thin pieces
	1.619	94.6	25.40	7.22 ± 0.20[5]	Witness plate holed and cracked Case fragmented into small pieces

1. Theoretical maximum density (TMD) = 1.712 gm/cm³
2. LVSD (2.76 ± 0.08mm/us for HBCNQ and 2.71 ± 0.05mm/us for SNQ)
3. Run up to constant velocity detonation was approximately 254mm
4. Run up to constant velocity detonation was approximatey 203mm
5. Constant velocity detonator for entire length of charge
6. Constant velocity detonation not achieved by last pin; however, witness plate damage and fragmentation characteristics are consistent with a go.
7. Run up to constant velocity detonation occurred by 203 mm. Pin data lost between 102 and 203 mm.
8. Run up to constant velocity detonation occurred by about 152 mm. Pin data lost between 102 and 152 mm.

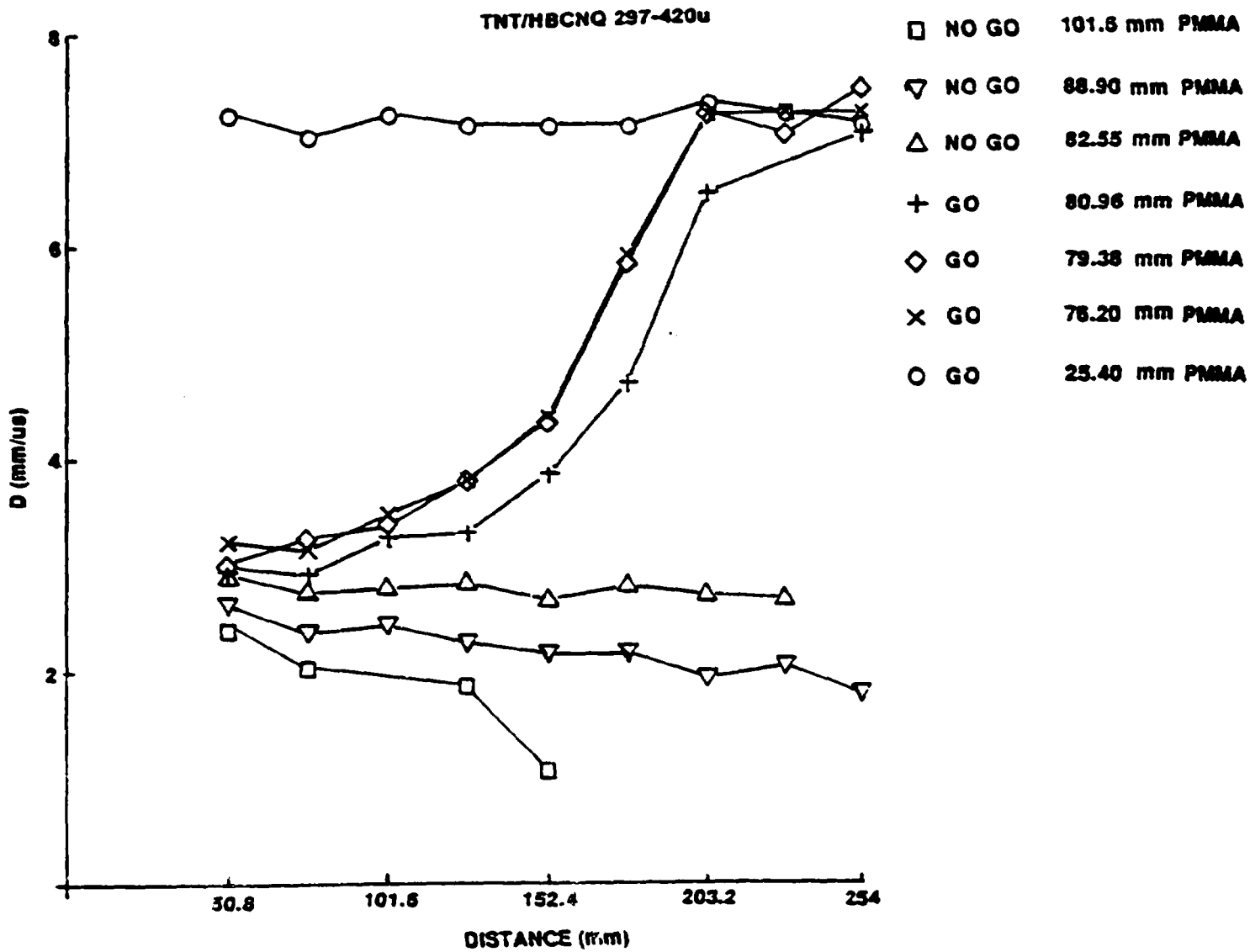

Figure 25. Modified ELSGT Results for TNT/HBCNQ (297-420 u)

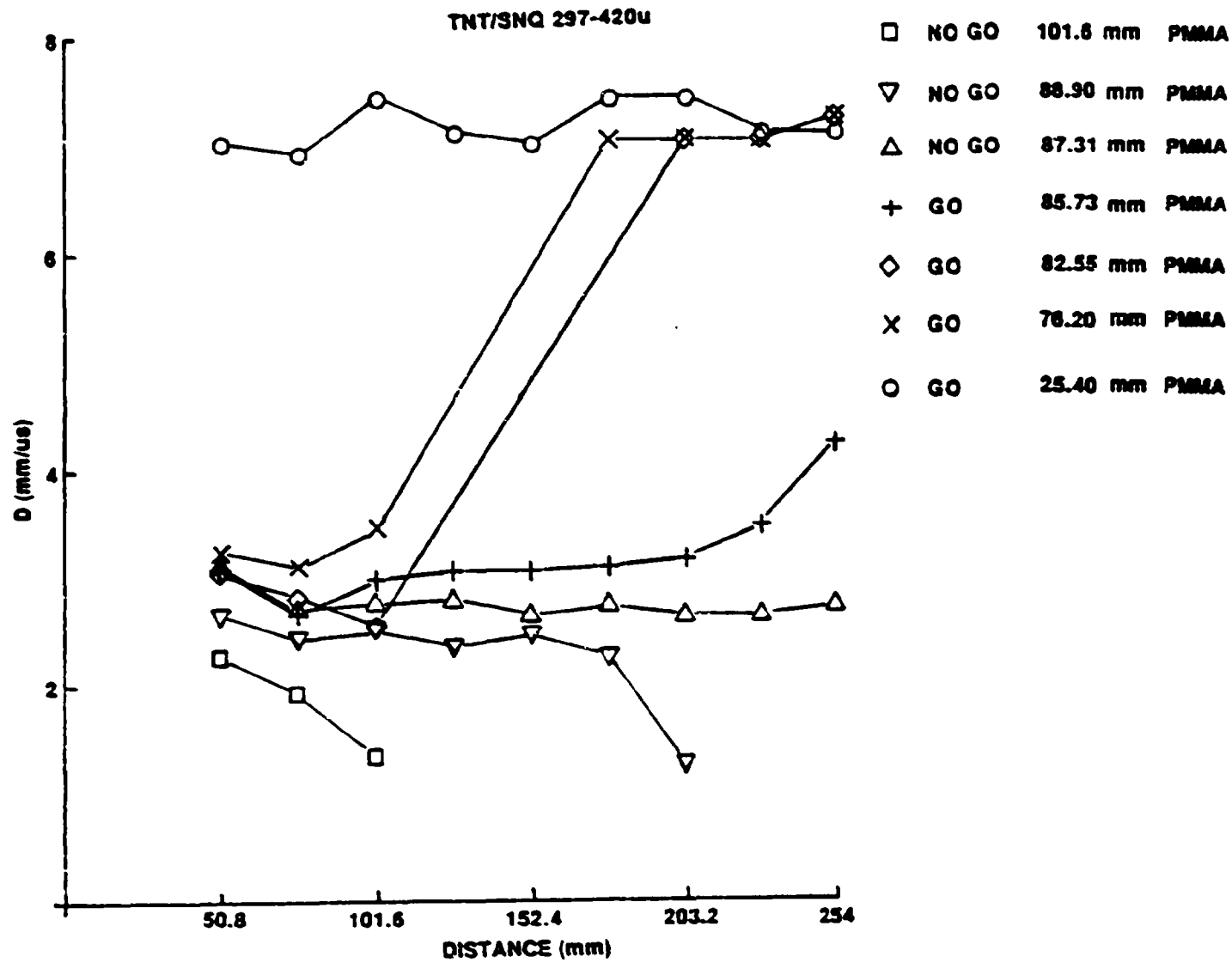

Figure 26. Modified ELSGT Results for TNT/SNQ (297-420 u)

occurred between 85.72 (Go) and 87.31 (No Go) mm of PMMA based on both pin and standard witness plate damage data. These thicknesses correspond to 32.8 and 31.5 kbar of input pressure, respectively.

b. TNT-NQ Series (105-210 micron NQ)

The results from the modified ELSGT series for the TNT/NQ (105-210 micron) melt cast system are summarized in Table 5 and run to detonation curves are shown in Figures 27 and 28. HBCNQ yields a 50 percent gap thickness between 84.14 (Go) and 85.72 (No Go) of PMMA based on pin data and the size of the case fragments. These thicknesses correspond to 34.4 and 33.2 kbar of input pressure, respectively. The 50 percent gap thickness for SNQ was not obtained during this test series. The data suggest a thickness less than 76.20 mm (42.1 kbar) will be required. One low density charge (92.4 percent TMD) achieved a constant velocity detonation after approximately a 127 mm run up.

c. RDX-NQ Series (210-297 micron NQ)

The results from the modified ELSGT series for the RDX/NQ melt cast system are summarized in Table 6 and run to detonation curves are shown in Figures 29 and 30. The system with HBCNQ yields a 50 percent gap thickness between 79.38 (Go) and 80.90 (No Go) mm of PMMA based on run-to-detonation data. These thicknesses correspond to 38.9 and 37.5 kbar of input pressure, respectively. The Corresponding 50 percent gap thickness for the system with SNQ was the same as that for HBCNQ. In this case, the Go/No Go point was based both on run-to-detonation data and witness plate damage.

5. SLOW COOKOFF (Generic Hardware)

Slow cookoff results are described in detail in Reference 3. The results from valid tests are summarized in Table 7 for convenience of the reader.

TABLE 5. MODIFIED ELROY RESULTS FOR TNT/NQ MELT CAST SYSTEMS (105-210 micron NQ)

Type NQ	Density (gm/cm³)	% TMD[1]	PMMA Thickness (mm)	Velocity (mm/us)	Comments
HBCNQ	1.642	95.9	101.6	No Go	Witness plate deformed about 51mm Case broken into large pieces
	1.646	96.1	88.90	No Go	Witness plate deformed about 89mm Case broken into large pieces
	1.653	96.6	85.72	No Go	Witness plate deformed about 51mm Case broken into large pieces
	1.645	96.1	84.14	2.85 ± 0.04[2]	Small diameter hole pushed through witness plate Case broken into medium-sized pieces
	1.651	96.4	82.55	2.89 - 3.43[3]	Witness plate holed and broken into 4 pieces Case broken into large pieces
	1.639	95.7	76.20	7.26 ± 0.0[4]	Witness plate holed and broken in half Case broken into small fragments
	1.644	96.0	25.40	7.26 ± 0.12[4]	Witness plate holed and broken in half Case broken into small fragments
SNQ	1.643	96.0	101.60	No Go	Witness plate deformed about 13mm Case broken into 5 pieces, some explosive recovered
	1.643	96.0	88.90	No Go	Witness plate deformed about 19mm Case broken into large pieces, explosive recovered
	1.649	96.3	82.55	No Go	Witness plate deformed about 38mm Case broken into large pieces
	1.653	96.6	79.38	Pin data lost	Witness plate deformed about 76mm Case broken into large pieces
	1.683	98.3	77.85	3.04-2.73[5]	Witness plate deformed about 76mm Case broken into large pieces
	1.64'	95.9	76.20	3.17-2.63[5]	Witness plate deformed about 89mm Case broken into medium-size pieces
	1.640	95.8	76.20	3.30-3.00[5]	Witness plate deformed about 102mm Case broken into large pieces
	1.581	92.4	76.20	7.52 ± 0.06[6]	Witness plate holed and broken into 3 pieces Case broken into small fragments

1. TMD = 1.712 gm/cm³
2. Appears to be a LVSD (2.85 ± 0.04mm/us) for approximately 203mm, after which a velocity increase commences.
3. Constant velocity not achieved, varied from 2.89 to 3.43mm/us.
4. Appears to be a constant velocity detonation after approximately 178mm run up.
5. Detonation velocity slowly decreasing.
6. Appears to be a constant velocity detonation after approximately 127mm run up.

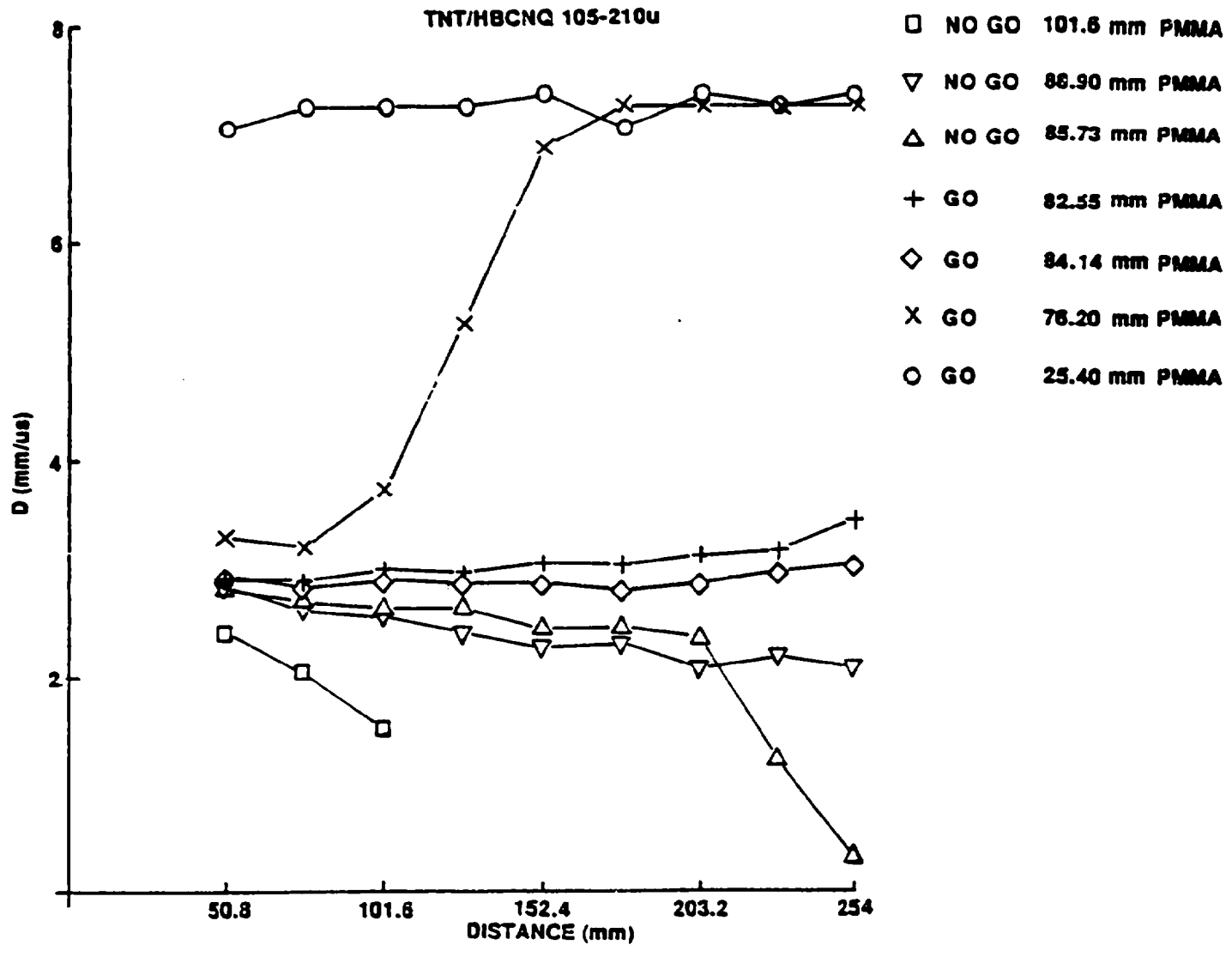

Figure 27. Modified ELSGT Results for TNT/HBCNQ (105-210 u)

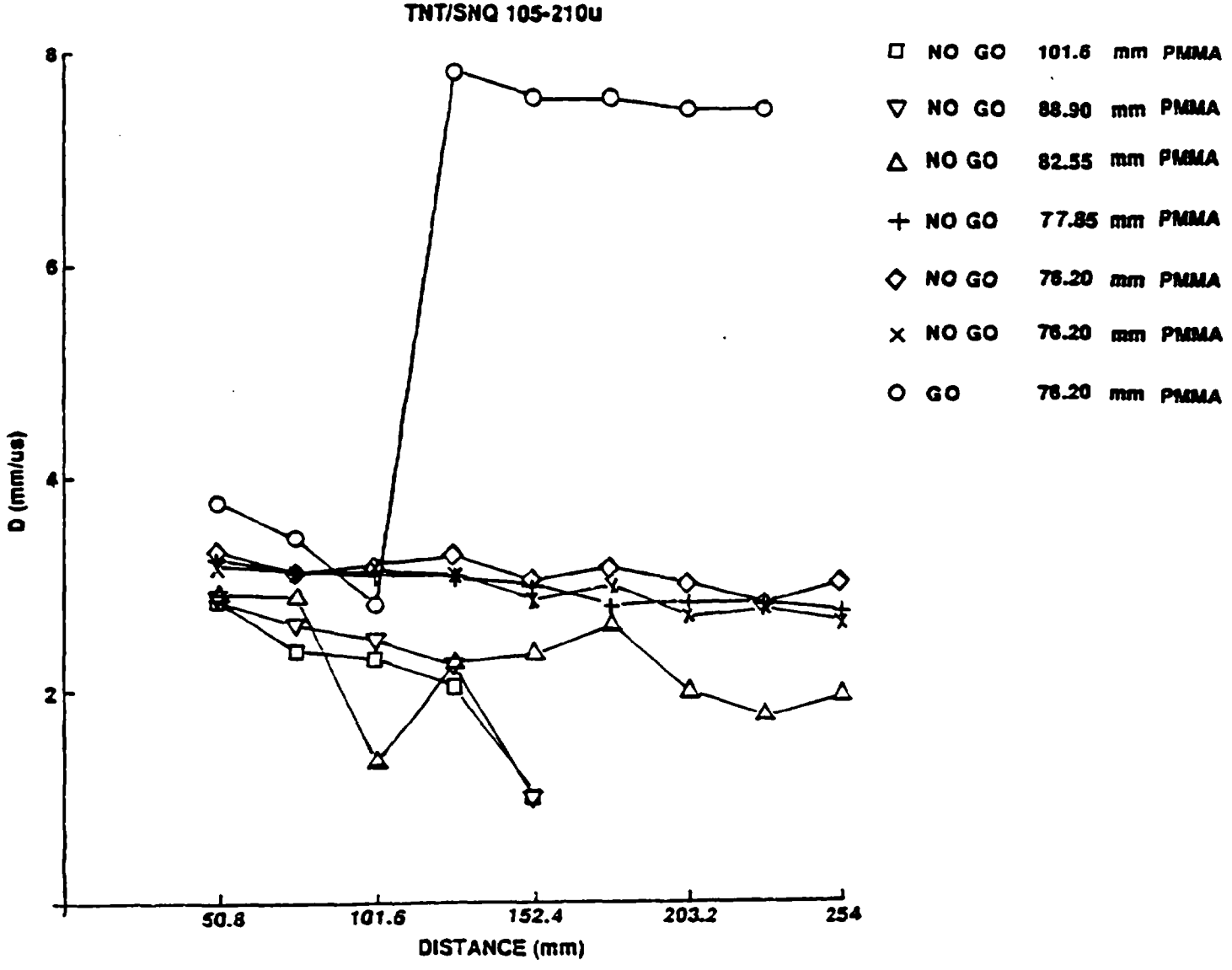

Figure 28. Modified ELSGT Results for TNT/SNQ (105-210 u)

TABLE 6. MODIFIED ELSOT RESULTS FOR RDX/NQ MELT CAST SYSTEMS

Type NQ	Density (gm/cm³)	% TMD[1]	PMMA Thickness (mm)	Velocity (mm/us)	Comments
HBCNQ	1.590	95.1	82.55	No Go	Witness plate not dented Case broken in half, some explosive recovered
	1.585	94.9	80.98	No Go	Witness plate not dented Case split on one side, most explosive recovered
	1.592	95.3	80.90	No Go	Witness plate not dented Case deformed and split about 5 inches on donor end, explosive recovered
	1.592	95.3	79.38	6.10 ± 0.08[2]	Witness plate dented and fractured into 3-4 pieces No hole; fragments relatively large
	1.581	94.6	79.38	6.03 ± 0.07[2]	Witness plate holed and shattered into 6 pieces Fragments ranged from small to large
	1.592	95.3	76.20	6.07 ± 0.09[2]	Witness plate dented with small hole in center, broken into 6 pieces Fragments were relatively large
	1.592	95.3	50.80	6.06 ± 0.07[2]	Witness plate holed and broken into 3 pieces Fragments medium to small
BNQ	1.621	97.0	88.90	No Go	Witness plate deformed slightly Case intact, all explosive recovered
	1.621	97.0	82.26	No Go	Witness plate not dented Case broken into at least 4 large pieces, no explosive recovered
	1.613	96.5	80.98	No Go	Witness plate not dented Case split into several large pieces
	1.617	96.8	79.38	6.16 ± 0.09[3]	Witness plate holed Case in small, thinned pieces
	1.609	96.3	76.20	6.68[4,5]	Witness plate holed Case in small, thinned pieces
	1.616	96.7	25.40	7.52 ± 0.11[6]	No data

1. TMD = 1.671 g/cm³
2. Constant velocity detonations
3. Appears to have reached constant velocity detonaton after approximately 152mm run up
4. Constant detonation velocity suggested after 229mm of runup
5. Additional charge length required to confirm constant velocity detonation
6. Appears to have reached constant velocity detonation after approximately 178mm run up

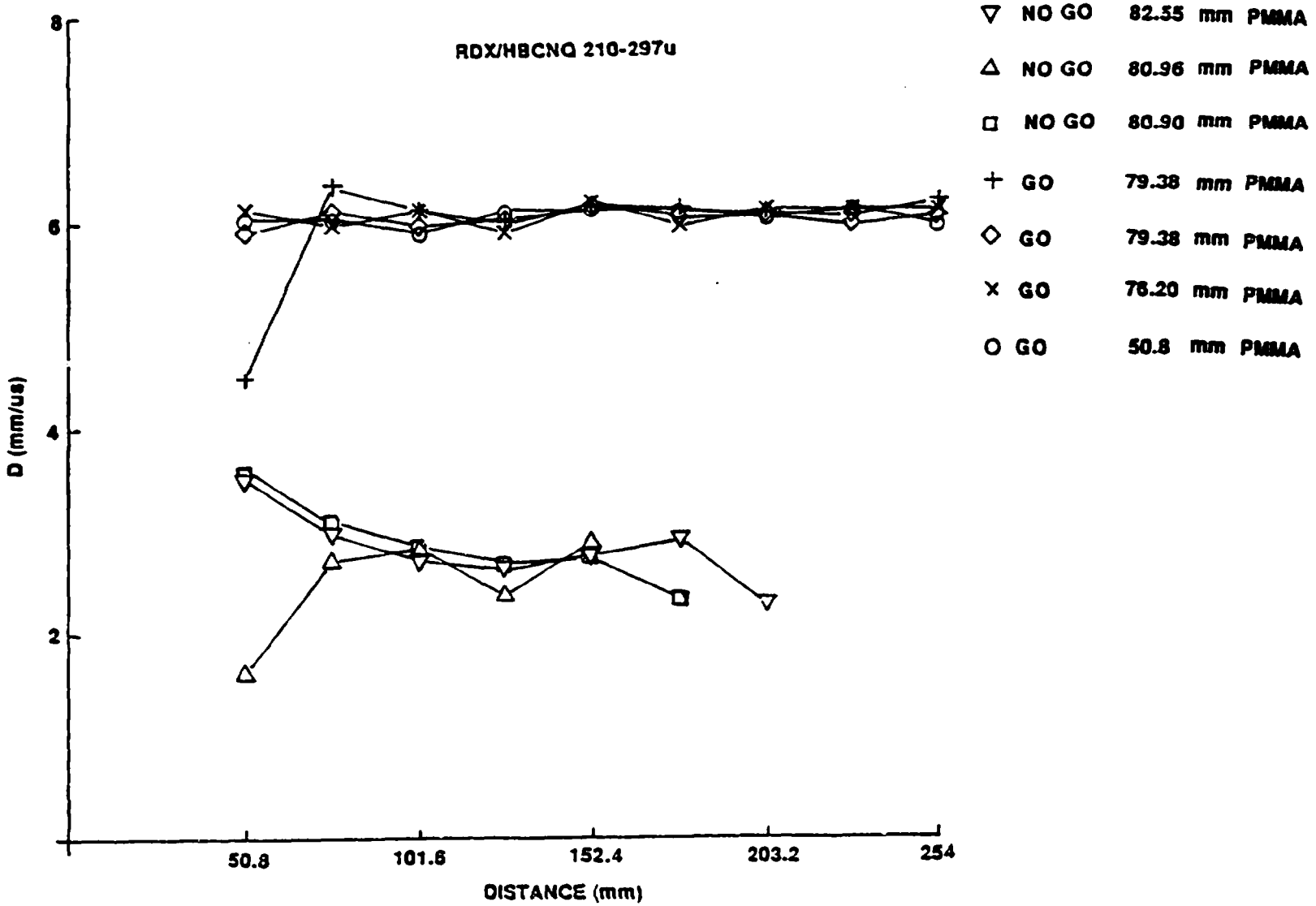

Figure 29. Modified ELSGT Results for RDX/HBCNQ (210-297 u)

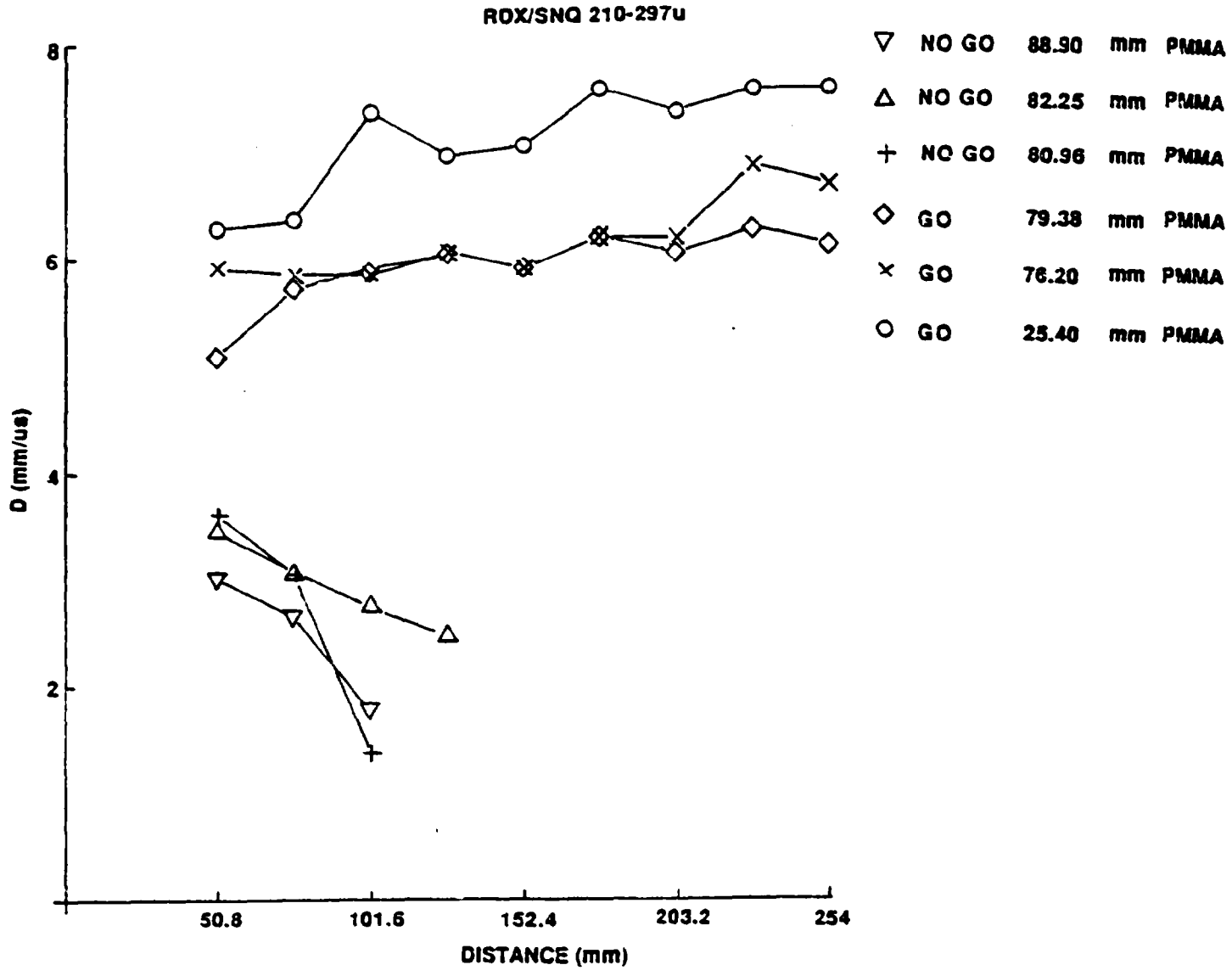

Figure 30. Modified ELSGT Results for RDX/SNQ (210-297 u)

TABLE 7. SLOW COOKOFF (GENERIC HARDWARE) TEST RESULTS

Formulation[1]	Test No.	Test Item	Reaction Time (hr/min)	Average Reaction Temperature (°C) Bomb Skin	Air Gap	Predicted[2]	Results[3]
HBCNQ(50)	4	1	15:15	145	144	185	PD
		2	16:26	147	146	185	PD
		3	21:19	152	162	185	PD
SNQ(50)	2	1	21:12	161	159	210	PD
		2	24:31	161	169	210	B
		3	32:28	177	202	210	E
HBCNQ (140)	7	1	17:10	150	151	183	PD
SNQ (140)	5	1	19:45	158	159	207	PD
		2	20:10	158	160	207	PD
		3	21:01	158	161	207	PD
HBCNQ (70)	3	1	24:34	146	148	187	B
		2	25:57	142	144	187	B
		3	27:24	140	148	187	B
SNQ (70)	6	2	31:05	160	159	200	B

1. Formulations coded as in Reference 3. HBCNQ(50) = TNT/HBCNQ (297-420 u), SNQ(50) = TNT/SNQ (297-420 u), HBCNQ (140) = TNT/HBCNQ (105-210 u), SNQ (140) = TNT/SNQ (105-210 u), HBCNQ (70) = RDX/HBCNQ (210-297 u) and SNQ (70) = RDX/SNQ (210-297 u).

2. Predicted values are extrapolated from curves obtained from variable heating rate experiments and are expected to be high and therefore only approximate. The values used in Reference 3 are not correct due to errors in the original variable heating rate calculations.

3. PD = partial detonation, E = explosion, B = burn. These descriptions are listed in decreasing order of violence as defined in Reference 3.

6. SLOW COOKOFF (SCO Units)

The results from experiments in small-scale cookoff units are summarized in Table 8. The entries in the results column are explained in Table 9.

7. BULLET IMPACT

Bullet impact results are described in detail in Reference 3. The results are summarized in Table 10 for convenience of the reader.

TABLE 8. SLOW COOKOFF TEST RESULTS (SCO Units)

Formulation		Weight of Explosive (gm)	Time (min) Self-Heating	Time (min) Max Reaction	Temperature (°C)[1] Oven	Temperature (°C)[1] Exp. at Self-Heating	Temperature (°C)[1] Exp. at Max Rxn	Results[2]
TNT/HBCNQ (297-420 u)	a	452.4	498	706	144	130 (157)	173	E[3]
	b	452.2	521	678	143	133 (157)	156	PD[4]
	c	455.0	467	654	141	131 (157)	161	PD
TNT/SNQ (297-420 u)	a	454.2	868	1034	162	147 (202)	180	Mild Def[5]
	b	454.1	877	951	158	151 (202)	191	B
	c	453.2	877	956	159	151 (202)	184	B
TNT/HBCNQ (105-210 u)	a	459.9	597	742	146	135 (158)	164	E
	b	459.1	697	710	144	130 (158)	147	PD
	c	459.0	525	698	144	133 (158)	156	PD
TNT/SNQ (105-210 u)	a	460.7	503	587	154	144 (201)	200	Def[6]
	b	457.7	735	833	152	144 (201)	203	E
	c	458.0	739	866	153	142 (201)	159	PD[4]
RDX/HBCNQ (210-297 u)	a	436.0	437	598	138	128 (157)	164	B
	b	436.0	369	562	136	124 (157)	144	Mild Def
	c	439.0	468	614	139	129 (157)	156	B
RDX/SNQ (210-297 u)	a	433	732	803	150	145 (197)	169	B[7]
	b	433	779	845	152	144 (197)	161	Mild Def
	c	433	735	778	149	144 (197)	151	Mild Def

1. Values in parentheses are predicted self-heating temperatures calculated from variable heating rate experiments using exotherm onset temperatures
2. E = explosion, PD = partial detonation, Mild Def = mild deflagration, B = burn
3. Temperature controller experienced periods of inconsistent function
4. Power failure on initial start up
5. O-ring inadvertently not included in upper container seal
6. Temperature held at 120°C instead of 105°C
7. Heater fan stopped prior to end of test

TABLE 9. DEFINITION OF REACTIONS SEEN IN SCO TESTS

1. Partial Detonation (PD) - Case broken into many small pieces and some bluing evident. Witness plate not holed.

2. Explosion (E) - Case broken into many small and large pieces.

3. Deflagration (Def) - Case broken into a few large pieces.

4. Mild Deflagration (Mild Def) - Case split, but remains in one piece.

5. Burn (B) - SCO unit top ruptured and contents vented.

Table 10. Bullet Impact Test Results

Test	Formulation[1]	Test Item	Explosive Weight (gm)	Results[2]
1	SNQ (50)	1	8423.4	Burn
2	SNQ (50)	1	8486.9	Burn
	HBCNQ (50	2	8491.4	Burn
3	HBCNQ (50)	1	8781.7	No Reaction
	SNQ (140)	2	8582.1	Burn
4	SNQ (140)	1	8355.3	Burn
	HBCNQ (70)	2	8604.8	Burn
	HBCNQ (70)	3	8595.7	Burn
5	HBCNQ (140)	1	8736.3	No Reaction
	HBCNQ (140)	2	8799.8	Burn
6	SNQ (70)	1	8387.1	Burn
	SNQ (70)	2	8740.9	Burn

1. Formulations coded as in Reference 3. HBCNQ(50) = TNT/HBCNQ (297-420 u), SNQ(50) = TNT/SNQ (297-420 u), HBCNQ (140) = TNT/HBCNQ (105-210 u), SNQ (140) = TNT/SNQ (105-210 u), HBCNQ (70) = RDX/HBCNQ (210-297 u) and SNQ (70) = RDX/SNQ (210-297 u).

2. Burn is defined as the process where the ordnance energetic material undergoes combustion. During this reaction, the ordnance case may open up and vent. The item remains in position although it may fall due to structural failure. The burning reaction presents no hazard to fire-fighting capability.

SECTION IV

DISCUSSION

The DSC thermograms associated with HBCNQ and SNQ suggest the former material is less stable than the latter (see Figures 9, 10, 11, and 12). Not only does the entire exotherm area occur at a lower temperature, but the main exotherm is preceded by a low intensity exotherm that covers a temperature range of about 40°C. The SNQ exotherm, on the other hand, is consistently preceded by an endotherm which is interpreted as the onset of melting and an indication of purity. The HBCNQ thermal characteristics are also reflected in the TNT-based formulations where the initial exotherm, attributed to HBCNQ, can be separated into two peaks at low heating rates. This initial exotherm, when associated with the TNT/SNQ formulation, is relatively sharp at all heating rates. The reduced thermal stability of HBCNQ may result from impurities probably incorporated during the recrystallization process that yields this particular high density, crystal habit. This is believed to be a reasonable assumption, since the DSC thermograms resulting from needle-like NQ (starting material for all recrystallizations) and SNQ are similar and are interpreted to suggest a degree of higher purity. These differences in thermal stabilities are clearly reflected in the activation energies where that for HBCNQ is about 10,000 cal/mole less than that for SNQ. The unique spherical shape does not appear to affect the results as crushed SNQ gives an apparent activation energy similar to that of uncrushed material. This thermal stability difference is also carried over into both the TNT- and RDX-based formulations where the formulation with SNQ always exhibits the higher apparent activation energy.

Critical diameters were determined for the four TNT-based and the RDX/HBCNQ formulations. The specific values are shown in Table 2. The values for the TNT/HBCNQ formulations are consistent with those for the comparable formulations containing SNQ in that the critical diameters are

smaller for the formulations with the smaller particle size NQ. The critical diameter for the TNT-based formulation containing SNQ (297-420 u) is smaller than that for the equivalent formulation with HBCNQ. Both TNT-based formulations with the NQs of smaller particle size had critical diameters less than 19 mm, the minimum diameter of the tapered section of the cone. Finally, the critical diameter for the RDX/HBCNQ formulation, with the NQ of intermediate particle size range, is close to that of the TNT/SNQ (297-420 u) formulation.

The more interesting and useful information gained from these critical diameter experiments comes from the regression analysis of the linear piezoelectric pin response data. These data are presented graphically in Figures 20, 21, 22, 23, and 24. Input pressure for all of these charges was that of Composition B (approximately 295 kbar). The slopes of the linear fits of the detonation velocities of all the charges, when plotted versus reciprocal radius, exhibit a negative trend to varying degrees thus suggesting that a diameter effect may be in operation below 76mm. Detonation velocities at a diameter of 50.8 mm were calculated for each formulation using the equations generated by the regression analyses. These values are shown graphically in Figure 31 and in Table 2. These data suggest that (1) both TNT-based charges containing SNQ are at or near ideal performance at a diameter of 50.8 mm, while all of the charges containing HBCNQ are performing below ideal, and (2) the diameter effect associated with the lone RDX-based formulation is much more pronounced than with the TNT-based formulations. No performance differences can be attributed to NQ particle size.

Detonation velocity/pressure experiments were designed and carried out based on critical diameter data obtained from cone experiments. Critical diameters were delineated by the cone experiments and were found to be generally consistent with data generated from the cylinders of varying diameters used in these detonation velocity/pressure tests. These data are

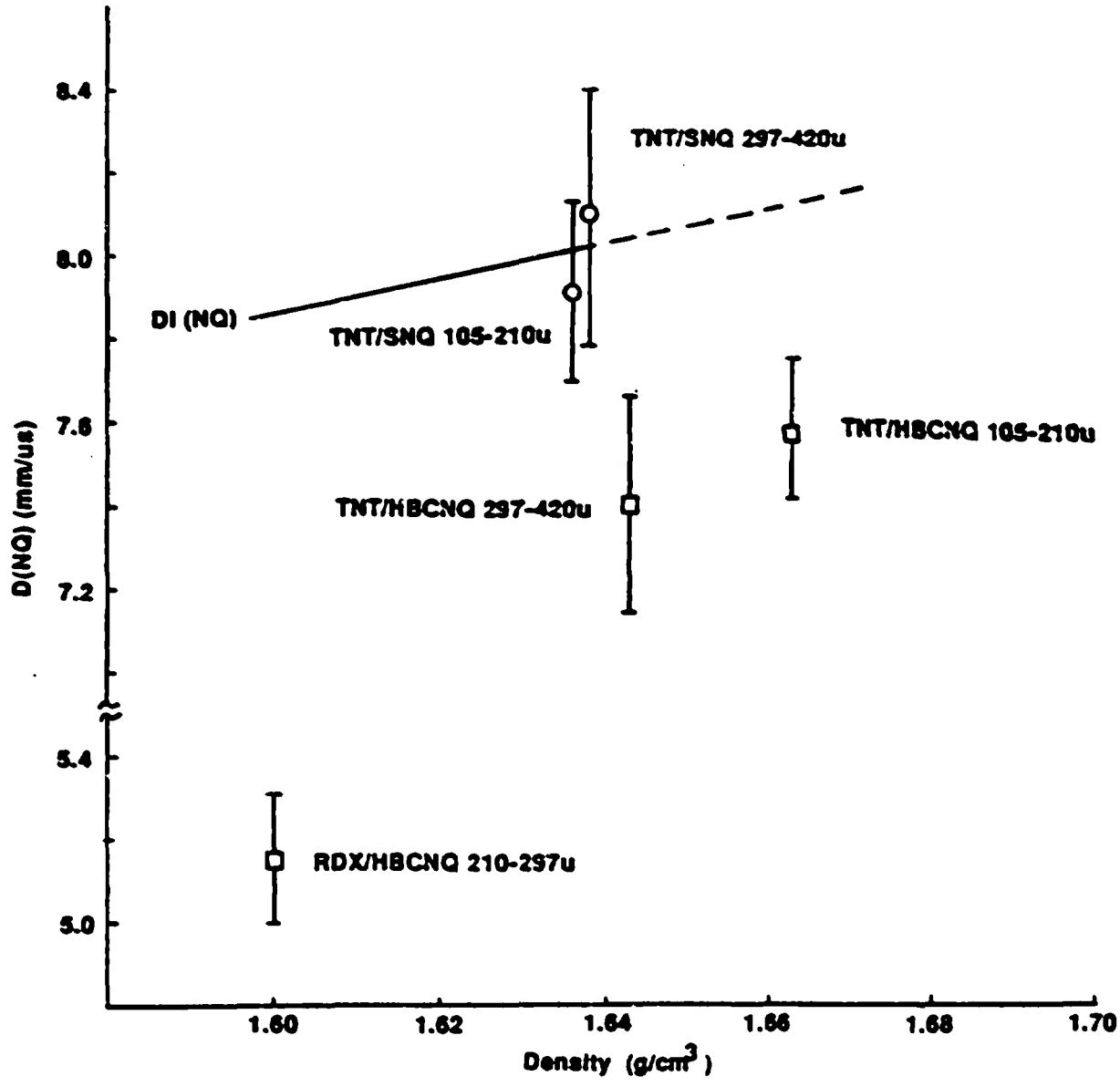

Figure 31. Calculated D(NQ) from Critical Diameter Experiments at a Diameter of 50.8 mm

shown in Table 11. The average detonation velocities for these cylindrical charges and their corresponding D(NQ) values are summarized in Table 3 and shown graphically in Figures 32, 33, and 34, along with the ideal curves for NQ. It is apparent from an inspection of the graphical display of these data that a diameter effect on the NQ detonation velocity, D(NQ), is in operation and that it is much more pronounced for the RDX-based formulations. More subtle is a suggested particle size effect within a given NQ crystal habit with D for the formulation with the smaller particle size greater than that for the formulation with the larger. The D(NQ) values from Table 3 for the 50.8 mm diameter, TNT-based cylinders were corrected to a density of 1.63 g/cm^3 using the ideal equation for NQ (Di = 1.44 + 4.015ρ). This manipulation yielded D(NQ) values for the formulation with SNQ (105-210 u), SNQ (297-420 u), HBCNQ (105-210 u), and HBCNQ (297-420 u) of 7.62 $\pm$ 0.03, 7.26 $\pm$ 0.15, 7.37 $\pm$ 0.13, and 7.13 $\pm$ 0.01 mm/us, respectively. The difference between the D(NQ) values for the smaller and larger particle sizes for a given crystal habit was calculated to be 4.7 and 3.3 percent for SNQ and HBCNQ, respectively. This calculation was based on the mean velocities. A review of the data presented in Figure 31, derived from conical configurations, shows consistency with the cylinder data for the TNT/HBCNQ formulations in terms of NQ performance, but not with the cylinder data from TNT/SNQ formulations. This is believed to reflect the tendency of the cone to promote an exaggerated detonation velocity and the special characteristic of SNQ to achieve ideal performance more easily than HBCNQ.

The detonation pressures for the TNT-based formulations with HBCNQ (105-210 u) and (297-420 u) and SNQ (105-210 u) vary randomly between 205 and 215 kbar with average values of 209 $\pm$ 5, 209 $\pm$ 2, and 211 $\pm$ 2 kbar, respectively. The average detonation pressure for TNT/SNQ (297-420 u) was 218 $\pm$ 2 kbar. The similarity of these detonation pressures is consistent with the similarity in detonation velocities (D and D(NQ)) of the charges

Table 11. CRITICAL DIAMETER DATA FROM CONE AND DETONATION VELOCITY/PRESSURE TESTS

Formulation	Particle Size (u)	Critical Diameter (mm) Cone	Cylinder
TNT/HBCNQ	105-210	<19	Between 25.4 - 50.8
TNT/HBCNQ	297-420	29 ± 3	Between 25.4 - 50.8
TNT/SNQ	105-210	<19	Approx. 19.05
TNT/SNQ	297-420	25 ± 3	Between 19.05-25.4
RDX/HBCNQ	210-297	24 ± 3	Less than 25.4
RDX/SNQ	210-297	ND[1]	Less than 25.4

1. Not determined.

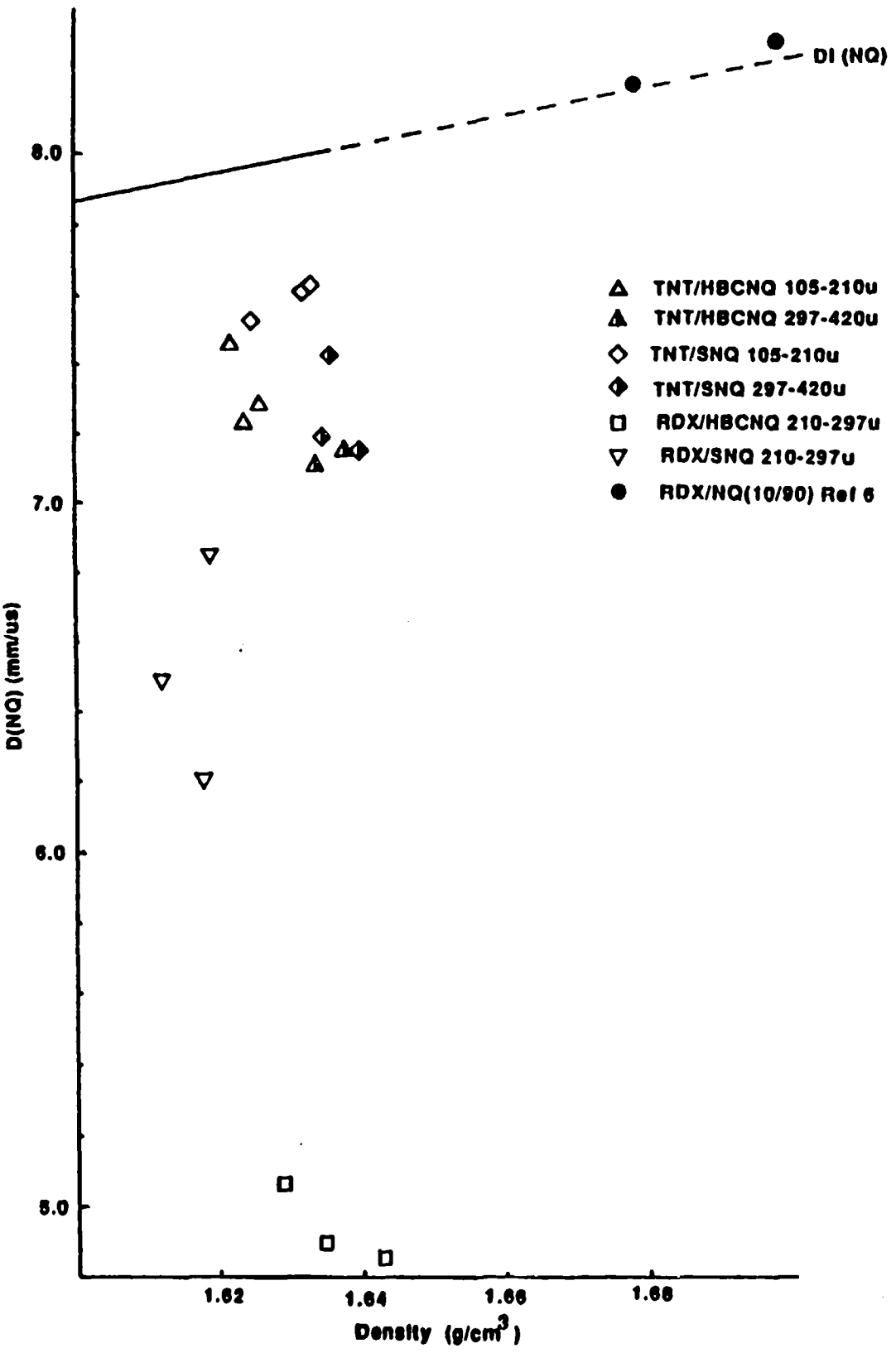

Figure 32. D(NQ) Versus Density for 50.8 mm Diameter Unconfined Cylindrical Charges

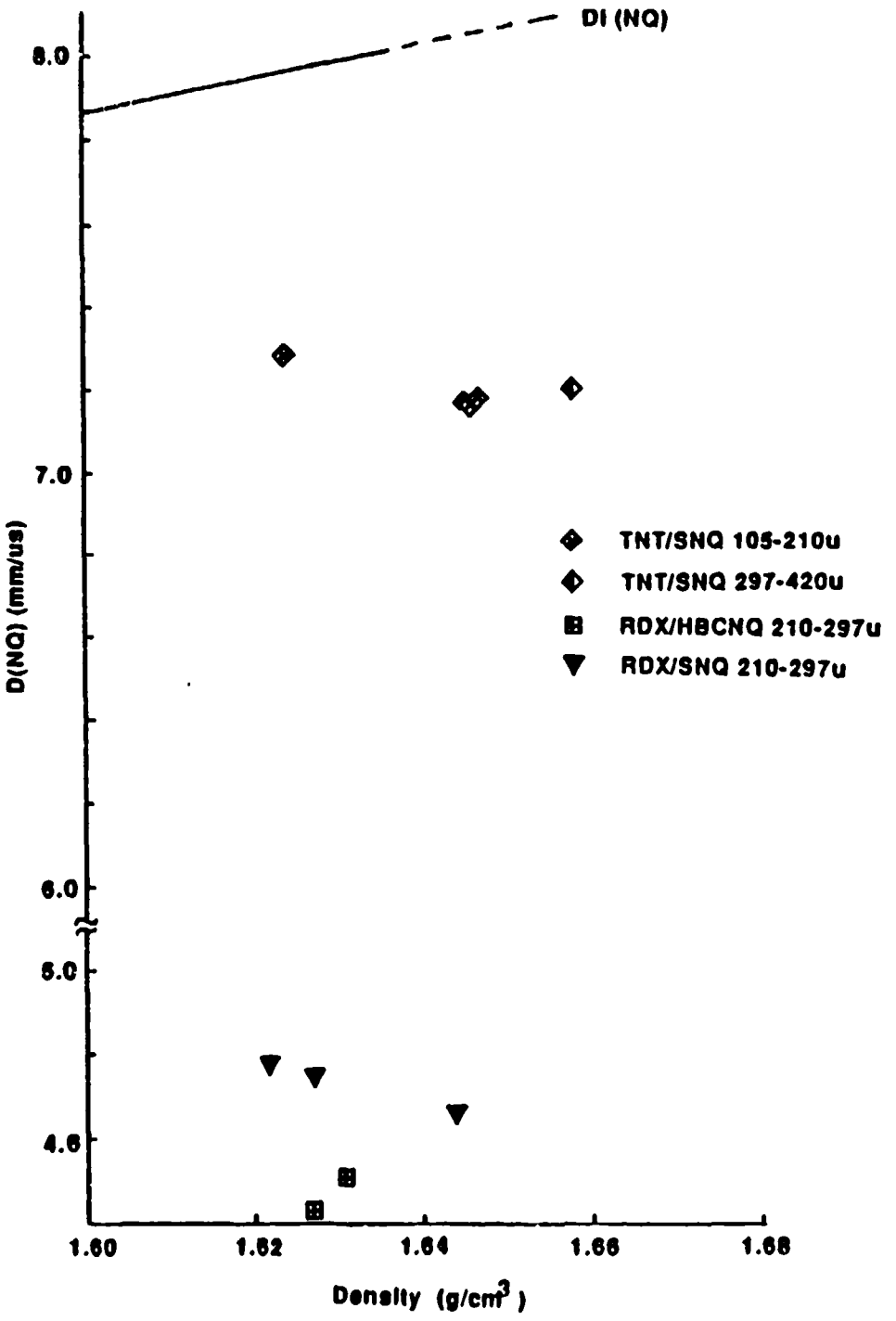

Figure 33. D(NQ) Versus Density for 25.4 mm Diameter Unconfined Cylindrical Charges

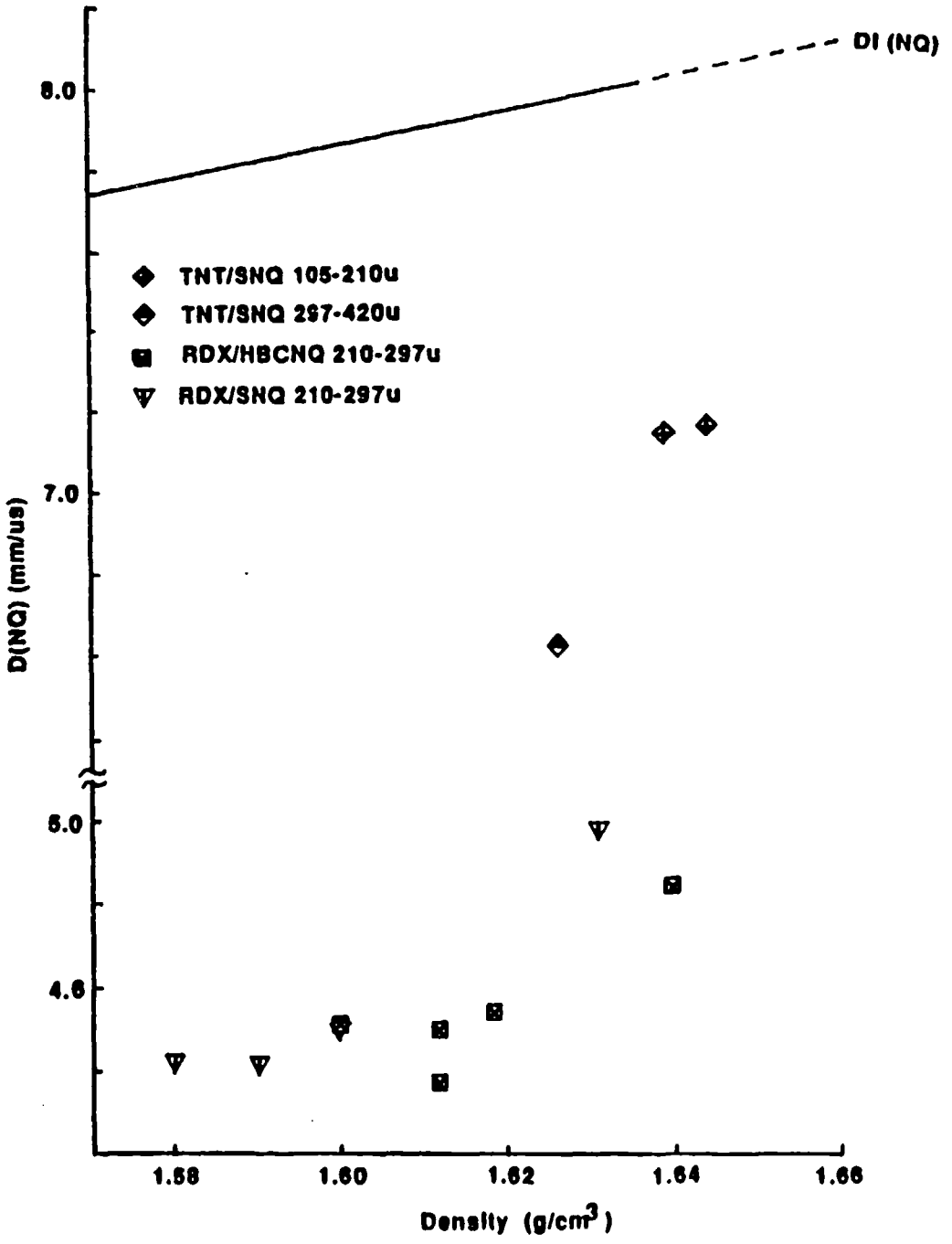

Figure 34. D(NQ) Versus Density for 19.05 and 38.1 mm Diameter Unconfined Cylindrical Charges

used for these measurements, which are shown to be influenced by a diameter effect at 50.8 mm (see Table 3 and Figure 32). The average detonation pressures for the RDX-based formulations with HBCNQ and SNQ were 66 $\pm$ 1 and 129 $\pm$ 15 kbar, respectively. These compare favorably with the corresponding average D(NQ) values of 4.94 and 6.52 mm/us.

The modified ELSGT was used to determine the test-specific shock sensitivities of TNT- and RDX-based NQ formulations. Detonation velocities were used to determine run-to-detonation distances in the acceptor charges and they, in turn, were used to assess the proximity to the initiation threshold. As found with other TNT-based formulations (Reference 2), detonations occurring near the 50 percent gap distance were characterized by relatively long run distances. The RDX-based formulation with SNQ exhibited similar characteristics, but the formulation with HBCNQ exhibited characteristics that were not seen with the TNT-based formulations. In only one case, for both the TNT- or RDX-based formulations, did the calculated D(NQ) values achieve the Di(NQ).

The TNT formulation with HBCNQ (297-420 u) yielded an apparent shock sensitivity of 37.3 kbar of input pressure. Witness plate damage supports this conclusion as a hole was punched through, and it was cracked. Case fragments were generally small. Data obtained from piezoelectric pins show that a constant velocity was not achieved by the last pin suggesting a run distance of greater than 254 mm. The charge receiving an input pressure of 35.9 kbar, while not achieving a detonation reaction considered to be high velocity during 279.4 mm of run, did appear to support a constant low velocity reaction (LVD) of 2.76 $\pm$ 0.08 mm/us. The LVD was not sufficiently powerful to significantly damage the witness plate under the charge as it was only deformed. The case damage was consistent with the above findings as it was fragmented into medium to large size pieces. The charges receiving 38.9 and 42.1 kbar of input pressure both experienced a run up to detonation of about 203 mm. In both cases the witness plates were holed,

deformed and cracked and the case walls fragmented into relatively small pieces. The charge receiving 123.3 kbar of input pressure sustained a constant detonation velocity of 7.20 ± 0.09 mm/us for the entire length of the charge. Witness plate damage for this charge was consistent with that of the charges receiving significantly less input pressure.

The corresponding formulation containing HBCNQ of a smaller particle size (105-210 u) achieved sufficient energy from an input pressure of 34.4 kbar to cut a small diameter hole through the witness plate. It was also deformed around 51 mm, but not cracked. Based on pin data, the reaction in the charge appeared to be a LVD (2.85 ± 0.04 mm/us) for approximately the first 203 mm of run distance. After this distance a slow velocity increase was observed; maximum velocity reached between the last two pins was 3.02 mm/us. The case fragments were of a medium size. The charge receiving 35.9 kbar of input pressure punched a normal size hole in the witness plate, as well as, broke it into four pieces. The run distance was at least 254 mm with a velocity of only 3.43 mm/us being reached between the last two pins. The velocity appeared to be very slowly increasing between the first and last pins. The case fragments from this charge were relatively large when compared to the charge previously described. The charges receiving 42.1 and 123.3 kbar of input pressure reached constant velocity detonations of 7.26 ± 0 and 7.26 ± 0.12 mm/us, respectively. The former charge experienced a run distance of 178 mm while the latter did not exhibit a measurable run distance. The witness plates associates with these charges were holed and broken in half and the case fragments were small.

The TNT/SNQ (297-420 u) charge receiving 32.8 kbar of input pressure exhibited a slowly increasing velocity over the entire measurable run distance. The velocity between the last two pins was 4.23 mm/us. The witness plate was holed and broken into 3 pieces and the case fragments were small. The charge receiving only 31.5 kbar input pressure supported an apparent LVD (2.71 ± 0.05 mm/us) for the entire charge length. The case

was fragmented into medium to large pieces and the witness plate was deformed about 76 mm, but was not holed or broken. The charges receiving input pressures of 35.9, 42.1, and 123.3 kbar supported detonation velocities of 7.13 $\pm$ 0.12, 7.11 $\pm$ 0.10 and 7.22 $\pm$ 0.20 mm/us, respectively. The first two charges reached constant velocities after run distances of around 203 and 152 mm, respectively, while the last charge exhibited no measurable run distance. Witness plates under these three charges were holed and broken into two or more pieces and case fragments were small. The charge receiving 42.1 kbar of input pressure was at a significantly lower density than the other charges in this series.

No constant velocity detonations were achieved with TNT-based charges containing SNQ (105-210 u) up to and including an input pressure at 42.1 kbar, where charge densities were maintained at 95.8 percent TMD or greater. A constant velocity detonation (7.52 $\pm$ 0.06 mm/us) was, however, achieved for a lower density casting (92.4 percent TMD) at 42.1 kbar of input pressure. The witness plate under the lower density charge was holed and broken into 3 pieces, whereas the plate under the higher density charge receiving the same input pressure was only deformed approximately 102 mm. The data clearly suggest that an input pressure greater than 42.1 kbar (76.2 mm of PMMA) will be required to bracket the 50 percent gap thickness for charges around 96 percent of TMD.

The data generated from this modified ELSGT series involving TNT-based charges containing NQ show the apparent 50 percent gap thicknesses to vary between a low of 32.8 and high of slightly greater than 42.1 kbar for charges in the 95 to 96 percent TMD range. For these given experimental conditions, there is approximately a 3 kbar difference between the charges containing HBCNQ that may be attributable to particle size. The data suggest the larger particle size HBCNQ is less sensitive. Furthermore, a closer inspection of the data shows that the formulation with the larger particle size is also at a slightly lower density than that with the smaller

particle size (95.3 versus 96.1 percent TMD). Experience shows that the lower density charge should be the more sensitive; therefore, it is believed the difference between charges of similar densities will be larger than 3 kbar. This finding is contrary to the norm. With charges containing particulate matter, the one with the material of smaller particle size will generally exhibit the lower shock sensitivity. This is the case with the charges containing SNQ, as the one containing the smaller particle size is observed to exhibit about a 10 kbar lower shock sensitivity.

Differences in shock sensitivity that may be attributable to NQ crystal habit vary from approximately 4.5 kbar for the formulations with the larger particle size NQ to approximately 7.7 kbar for the ones with the smaller particle size. In the case of the former, the formulation with HBCNQ is the less sensitive and for the latter the one with SNQ is the less sensitive. The densities of the charges used for these comparisons were similar. One possible explanation for this observed reversal in trends is that, given similar charge densities, the particle density of the larger size SNQ is less than that of the comparable size HBCNQ, while the particle density of the smaller size SNQ is greater than that of the comparable size HBCNQ. Clearly, all of these observed shock sensitivity differences are small and may be influenced by the known diameter effect and/or reflect the lack of statistical testing and reduced quality control in charge preparation.

The detonation velocities for those TNT-based charges considered to have achieved a constant value ranged from 7.11 $\pm$ 0.10 to 7.26 $\pm$ 0.12 mm/us with the exception of one lower density charge, TNT/SNQ (105-210 u), that achieved 7.52 $\pm$ 0.06 mm/us. These data are summarized in Table 12, along with D(NQ), percent Di(NQ) and input pressure values, and are presented graphically in Figure 35. These limited data have been critically analyzed, taking into consideration the density variation between charges, and suggest a charge diameter effect on D(NQ) is in operation at 73.2 mm for all but the lower density charge. There appears to be (1) a particle size effect on

TABLE 12. RELATIONSHIP OF D(NQ) TO OBSERVED DETONATION VELOCITIES FOR TNT/NQ FORMULATIONS

Type	Particle Size (u)	Density (g/cm^3)	Observed D(mm/us)	D(NQ) (mm/us)	% Di(NQ)[1]	Input P (Kbars)
HBCNQ	105-210	1.639	7.26 ± 0	7.37 ± 0	91.9	42.1
HBCNQ	105-210	1.644	7.26 ± 0.12	7.36 ± 0.24	91.5	123.3
HBCNQ	297-420	1.646	7.20 ± 0.09	7.23 ± 0.17	89.8	123.3
SNQ	297-420	1.618	7.13 ± 0.12	7.34 ± 0.24	92.5	35.9
SNQ	297-420	1.585	7.11 ± 0.10	7.34 ± 0.20	94.1	42.1
SNQ	297-420	1.619	7.22 ± 0.20	7.52 ± 0.12	94.7	123.3
SNQ	105-210	1.581	7.52 ± 0.06	8.17 ± 0.12	105	42.1

1. Percent of ideal detonation velocity for pure NQ at the given density

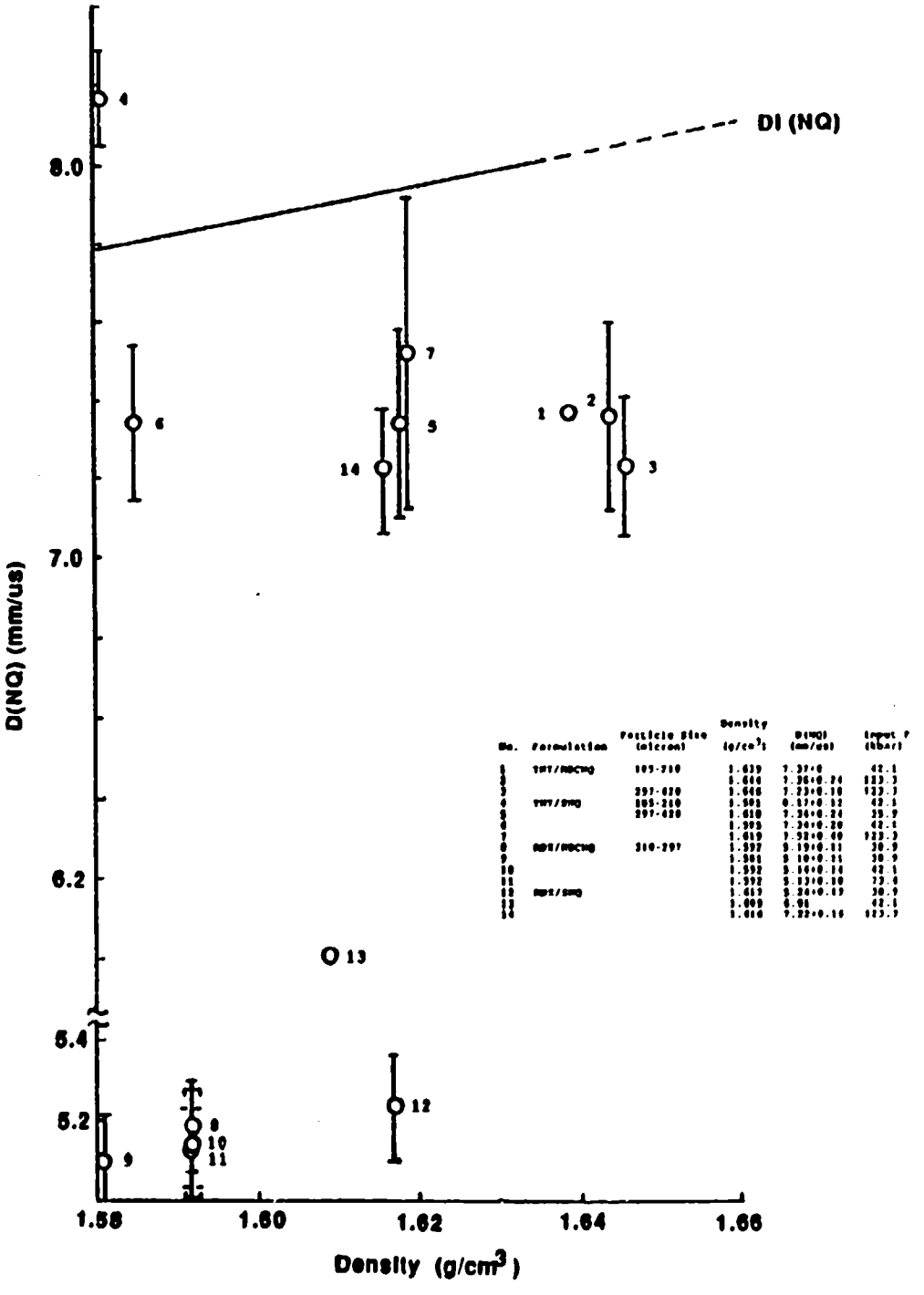

Figure 35. D(NQ) Versus Density for ELSGT Charges Achieving Constant Velocity Detonation

D(NQ) for the SNQ formulations and none on those with HBCNQ, and (2) no NQ crystal habit effect on D(NQ) for the 297-420 u formulations (large charge density variation precludes comment on the affect of NQ crystal habit for the 105-210 u formulations). The affect of input pressure on D(NQ) is not clear from the present data. These same subtle trends are apparent upon close inspection of the 50.8 mm diameter data shown in Table 3.

There was no distinction between the two crystal habits of NQ in the RDX-based formulation with respect to the input pressure required to initiate a constant velocity detonation. Both achieved constant velocity detonations at an input pressure of 38.9 kbar and failed to propagate at 37.5 kbar. The velocities associated with these detonation reactions were 6.10 $\pm$ 0.08 mm/us for the charge containing HBCNQ and 6.16 $\pm$ 0.09 mm/us for the other. These velocities correspond to percent Di(NQ) values of 66.3 and 66.1, respectively. While the witness plate under the charge containing SNQ was holed and the case fragments small and thinned, the plate under the charge containing HBCNQ was only dented and fractured into several pieces and the case fragments were relatively large. Other charges containing HBCNQ behaved similarly. Input pressures of 38.9, 42.1, and 73.4 kbar resulted in detonation velocities of 6.03 $\pm$ 0.07, 6.07 $\pm$ 0.09 and 6.06 $\pm$ 0.07 mm/us, respectively. All witness plates associated with these charges were holed and broken into multiple pieces and case fragments varied from large to small. These detonation velocities are similar to the calculated value for a diameter of 73.2 mm (6.14 mm/us) from the critical diameter experiment. These values are shown graphically as Di(NQ) versus charge density in Figure 35 and are summarized in Table 13. The data clearly suggest a diameter effect is in operation in that the D(NQ) values are similar and are unaffected by increasing input pressure.

The charges containing SNQ, on the other hand, respond differently to increasing input pressure. The charges receiving 42.1 and 123.3 kbar of input pressure, for example, achieved detonation velocities of 6.68 and 7.52

Table 13. RELATIONSHIP OF D(NQ) TO OBSERVED DETONATION VELOCITIES FOR RDX/NQ FORMULATIONS

Type	Density (g/cm^3)	Observed D (mm/us)	D(NQ) (mm/us)	% Di(NQ)	Input P (kbar)
HBCNQ	1.592	6.10 ± 0.08	5.19 ± 0.11	66.3	38.9
HBCNQ	1.581	6.03 ± 0.07	5.10 ± 0.10	65.5	38.9
HBCNQ	1.592	6.07 ± 0.09	5.14 ± 0.13	65.6	42.1
HBCNQ	1.592	6.06 ± 0.07	5.13 ± 0.10	65.5	73.4
SNQ	1.617	6.16 ± 0.09	5.24 ± 0.13	66.1	38.9
SNQ	1.609	6.68	6.01	76.1	42.1
SNQ	1.616	7.52 ± 0.11	7.22 ± 0.16	91.1	123.3

± 0.11 mm/us. These values were achieved after substantial run up and correspond to 76.1 and 91.1 percent of Di(NQ), respectively. These data are also shown graphically in Figure 35. Witness plates associated with these charges were cleanly holed and case fragments were small and thinned. While a diameter effect is also operational with these charges, it is apparent that it is sensitive to input pressure and, perhaps, can be eliminated at a smaller diameter than with those containing HBCNQ.

The major conclusion from the modified ELSGT series is that the data are influenced by the diameter of the test unit and all perceived differences in sensitivity attributed to NQ crystal habit must be so caveated. There are obvious differences in the measured data gleaned from this overall evaluation that can be realistically linked to crystal habit and these are pointed out throughout the text and again in the conclusion section.

Data generated at this facility prior to March, 1988, from eight-inch gap experiments with RDX-based formulations of similar composition to those used in this current study were consistent with the data generated from charges of only 73.2 mm charge diameter. See Tables 13 and 14. The charge containing HBCNQ achieved a D(NQ) value of 5.25 mm/us which corresponds to only 69 percent of Di(NQ). This finding suggests that the diameter effect on D(NQ) is still operational at a diameter of 175 mm, at least within the experimental condition of 35 kbar input pressure and 400 mm maximum charge length. For the charge containing SNQ, a D(NQ) value of 7.7 mm/us was achieved. This corresponds to 102 percent of Di(NQ). These values suggest the diameter effect is no longer operational even for an input pressure of only 35 kbar. This finding is not unexpected, as both the data generated from the cone experiments and the modified ELSGT experiments suggest the diameter effect will be eliminated at a charge diameter not much greater than 73-76 mm.

The slow cookoff test series using generic hardware suffered from

Table 14. RELATIONSHIP OF D(NQ) TO OBSERVED DETONATION VELOCITIES FOR RDX/NQ FORMULATION FROM EIGHT-INCH GAP EXPERIMENTS

Formulation[1]	Density (g/cm^3)	Observed[2] D (mm/us)	D(NQ) (mm/us)	% Di(NQ)	Input P (kbar)
RDX/HBCNQ	1.53	6.1	5.25	69	35
RDX/SNQ	1.51	7.7	7.65	102	35

1. RDX/NQ/Al/Polyethylene/lecithin (22/45/16/16.7/0.3), percent by weight
2. Inside diameter = 175 mm

repeated oven failures that rendered many tests invalid. As previously mentioned, thermocouples were located on the outside of the steel bomb casing. As a result, the temperature-time traces give virtually no indication of the temperature of the explosive away from the surface or of self heating. A quick inspection of the temperature data in Reference 3 shows that, in most cases, the bomb skin and airgap temperatures are similar. Therefore, the temperature-time traces appear to simply reflect the programmed ramp speed of 3.3°C per hour. As previously described, the test plan called for rapid heating to a preplanned temperature 55°C below the expected reaction temperature, a hold for 60 minutes, and then a programmed increase in temperature. The predicted reaction temperatures for the TNT- and RDX-based formulations were 170 and 130°C, respectively. This dictated hold temperatures of 115°C and 75°C, respectively. In the former case, the hold temperature is 35°C above the melting point of TNT (80°C) and about 30°C above the normal processing temperature for these formulations. The 60-minute hold is believed to be sufficient time for most of the TNT phase to have melted. Any reaction between TNT and NQ or impurity in NQ may be accelerated in this state and detectable in the results. For the latter case, the hold temperature is below the processing temperature and furthermore, the active ingredients will have remained in the solid state. After these tests were conducted, it was discovered that the predicted temperatures were incorrect due to errors made in the calculations resulting from the variable heating rate experiments. The predicted values shown in Table 7 are the corrected values.

Formulations with SNQ, regardless of particle size or medium, reacted with various degrees of violence when the average bomb surface temperature was in the range 158 to 161°C. There was one exception (test 2, test item 3) where the reaction occurred at a measured surface temperature of 177°C. The TNT formulations containing HBCNQ reacted when the average bomb surface temperatures were in the range 148 to 150°C,

regardless of particle size. The RDX-based formulation with HBCNQ reacted at an average bomb surface temperature of 143°C, while the single test with SNQ reacted at a bomb surface temperature of 160°C. The times shown in Table 7 reflect the ramp time to the hold temperature, the one-hour hold, and the programmed ramp time to reaction.

The data show that all of the formulations containing SNQ react at average bomb surface temperatures higher than those for the corresponding formulations with HBCNQ and that the RDX-based formulations, regardless of NQ crystal habit, react much less violently than the formulations based on TNT. No conclusions can be drawn from the TNT-based formulation test data based on NQ crystal habit or particle size. That the SNQ-loaded formulations react at the higher bomb surface temperature is consistent with their higher apparent activation energies.

The slow cookoff test series using SCO units differed, in part, from the series previously described in that the explosive weights averaged 456 g for the TNT formulations and 435 g for the RDX formulations, whereas the same formulations in the generic hardware tests averaged 2019 and 2159 g, respectively. Also, the SCO units were instrumented with an internal thermocouple centered in the explosive. This internal thermocouple allowed detection of the temperature at which self-heating was initiated and a more accurate representation of the temperature at which maximum reaction occurred. The self-heating temperature is characteristic of the explosive, whereas the the burst temperature may be highly influenced by the strength of the container.

The TNT/HBCNQ formulation, regardless of NQ particle size, exhibited similar end results when tested in SCO units, namely explosions and partial detonations. This finding was similar to that from the generic hardware cookoff tests, with the exception that all TNT/HBCNQ generic units yielded partial detonations. Self heating initiated at an average temperature of 132°C for both particle sizes and maximum reaction occurred in the

range 147-173°C. While times to self-heating and maximum reaction were fairly similar for the two NQ particle sizes, the smaller particle size material tended to exhibit slightly longer times. The predicted temperature for the initiation of self-heating for this formulation was consistently about 25°C higher than the measured temperatures.

The end results for the TNT/SNQ formulations were more varied, but the data suggest the formulation with the smaller particle size SNQ reacts more violently than a formulation with the larger particle size. This finding is similar to that seen in the generic hardware tests. The average temperature at which self-heating occurred was 150°C for the larger particle size and 143°C for the smaller. This is 11 to 18°C higher than for a formulation with HBCNQ and is consistent with the DSC data. The temperatures at which maximum reaction occurs are more varied but, in general, they are higher for the formulation with SNQ. The predicted temperature for the initiation of self-heating for this formulation was consistently 50-60°C higher than the measured temperatures.

Both types of NQ in the RDX formulations behaved similarly and, in general, less violently than the TNT-based formulation. This finding is consistent with that from the generic hardware. As seen with the TNT-based formulations, the RDX formulations with SNQ exhibited higher temperatures at the initiation of self heating (average delta was 17°C) than those with HBCNQ. Temperatures at maximum reaction were too varied to interpret. The times to self-heating were consistently lower for the HBCNQ formulations and the delta between the average times (309 min) was consistent with the relationship between the heating rate and the delta between the average temperatures at self heating.

The bullet impact test results are characterized by mild burns through the bullet holes for the RDX-based formulations and, generally, burns with loss of at least one end cap for the TNT-based formulations. The results suggest that both formulations, regardless of the type of NQ or its particle

size, respond rather mildly to bullet impact; however, the burns from the TNT-based formulations appear to be somewhat more intense than those from the RDX-based formulations. Those TNT-based formulations containing HBCNQ appear to be more stable to bullet impact than those containing SNQ.

SECTION V

CONCLUSIONS

DSC thermograms obtained from neat HBCNQ and SNQ suggest the former is less stable than the latter. This conclusion is reflected in the apparent activation energies for the thermal decomposition process where that for HBCNQ is about 10,000 cal/mole less than that for SNQ. It is believed the reduced thermal stability of HBCNQ results from impurities probably incorporated during the recrystallization process. As in the neat form, both the TNT- and RDX-based formulations containing HBCNQ exhibit lower apparent activation energies for the thermal decomposition process than similar compositions with SNQ. These data suggest NQ plays a major role in the decomposition process and, in so doing, those formulations containing HBCNQ are less stable thermally. This is further substantiated by the slow cookoff tests in SCO units where self-heating is initiated at lower temperatures for formulations containing HBCNQ. The influence of NQ particle size was minimal. End results were less definitive, since they are to a large extent governed by the strength of the test unit; however, it was apparent that RDX-based formulations behaved less violently than TNT-based formulations. Both types of formulations, regardless of type of NQ or particle size, respond mildly to bullet impact.

The TNT-based formulations with NQs of small particle size exhibited the smaller critical diameter (d_c) values. While these d_c values give an indication of the diameter at which the charge will no longer support sustained detonation and also offer some differentiation based on particle size, they do not, without further investigation, give any insight into the diameter, d_i, at which ideal detonation velocity, D_i, will be achieved by the particular formulation. The velocity D_i is defined as the volume weighted summation of the ideal velocity contributions of each of the energetic components of the formulation, $D_i = \sum aD_{i(1)} + bD_{i(2)} + \ldots + zD_{i(n)}$, where a, b,...z are the volume fractions and the terms 1,2,...n represent the

different components. Between d_c and d_i a constant velocity, non-ideal detonation with velocity D may be afforded, where $D < D_i$. D may be a function of charge diameter, NQ particle size, initiation pressure, confinement, and other ingredients of the formulation.

The measured detonation velocities for the formulations and the corresponding D(NQ) values, for both NQ crystal habits, from the detonation velocity/pressure and ELSGT experiments clearly showed that all but one of these values were less than ideal at or below a charge diameter of 73mm. These limited data also suggest that D_i(NQ) can be achieved more readily with SNQ than with HBCNQ and that this overall effect on D(NQ) is more pronounced in the RDX-based system.

It is believed this enhanced propensity towards ideal performance by SNQ when subjected to a shock environment may result, at least partially, from its greater internal porosity (inaccessible to continuous medium) per individual spherulite. This porosity may exist as rather large internal voids, an example of which is thought to be shown in Figure 36a and b, that sometimes appear near the center of the spherulite and sometimes on the surface as seen in Figure 37. It is believed the more important voids may be in the form of more uniform microporosity that exists within and between the individual crystallites emanating from the common center of each spherulite and the surface porosity not filled with the continuous medium. This porosity may act as sites for the generation of hot spots when subjected to the instantaneous high pressure of the traveling shock wave. The heat generated by the thermal decomposition reactions taking place at these hot spots strengthens the shock wave thus accelerating the overall decomposition process ultimately leading to a sustained detonation. While the particulate (NQ) density differences may help to explain the performance differences observed for the two crystal habits, it is further suggested that the other ingredients of the particular formulation may also significantly influence the performance of the NQ component.

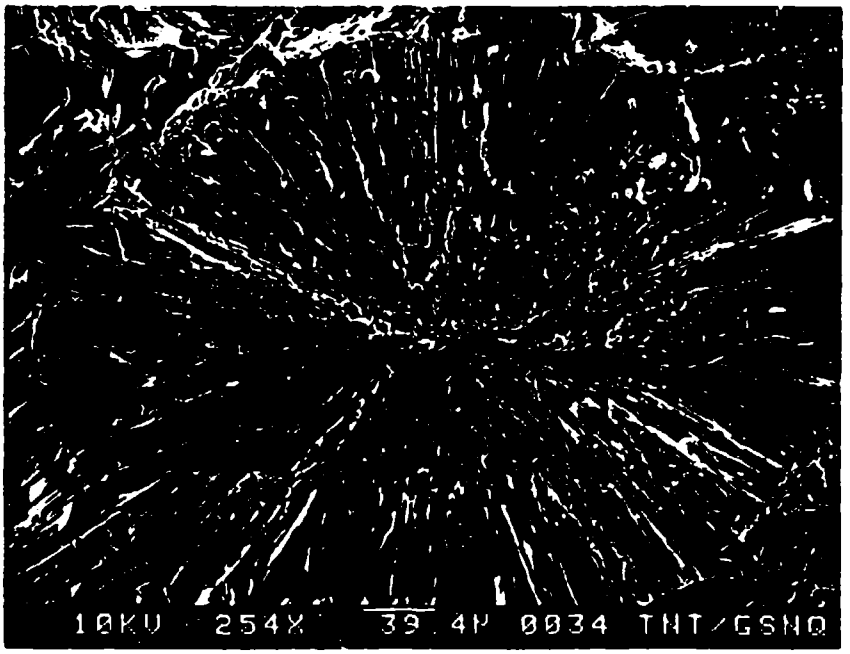

Figure 36. a. Scanning Electron Micrograph (254X) of Internal Porosity Located in an SNQ Spherulite.

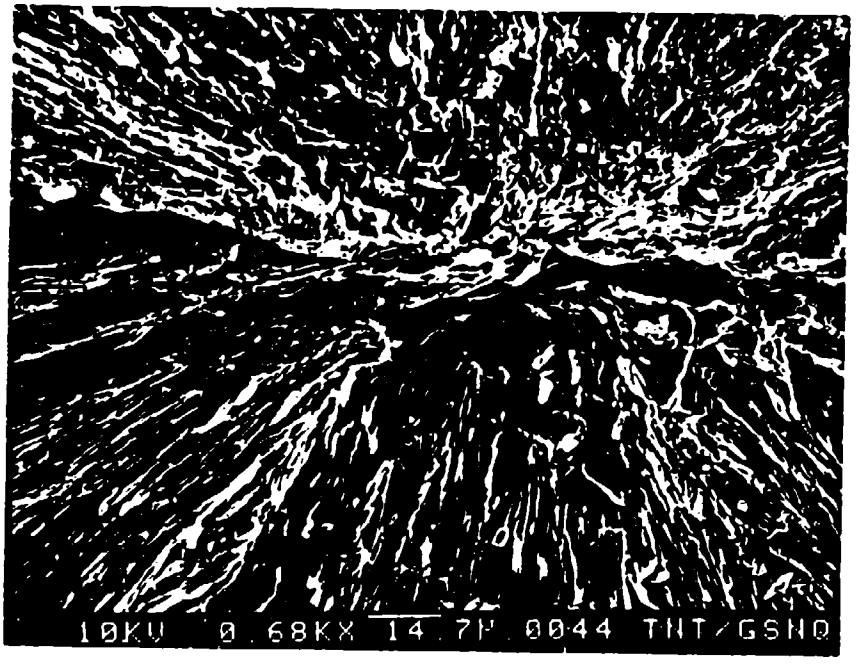

Figure 36.b. Scanning Electron Micrograph (680X) of Internal Porosity Located in an SNQ Spherulite

Figure 37. Scanning Electron Micrograph of Large Surface Void Located on an SNQ Spherulite

A review of the data in Tables 3 and 12, for the TNT-based formulation, reveals that the differences attributable to NQ crystal habit are small and that the deviations from Di(NQ) are also small when compared to similar values obtained from the RDX-based formulations. In this TNT medium there is only minimal distinction between particle sizes and minor influence on percent Di(NQ) attributable to input pressure or charge diameter between 50.8 and 73.2 mm. Percent Di(NQ) is influenced somewhat by charge diameter below 50.8 mm (formulations containing SNQ only). These findings, gathered from rather limited data, are initially interpreted to suggest that D(HBCNQ) may be apprcaching a maximum value that is medium dependent with little distinction attributable to particle size or input pressure. D(SNQ), on the other hand, appears to reflect some influence attributable to particle size and, perhaps, input pressure. Clearly, more experiments are required to quantify these initial conclusions.

A similar review of the data from Tables 3, 13, and 14 for RDX-based formulations reveals an entirely different NQ behavior with respect to medium and crystal habit. The deviations of D(NQ) from Di(NQ) range from 44 to 31 percent for HBCNQ over a diameter range of 25.4 to 175 mm and from about 31 to 9 percent for SNQ over a diameter range of 25.4 to 73.2 mm with one 175 mm diameter charge achieving ideal velocity. Input pressures were varied above a charge diameter of 50.8 mm and there was some charge density variation. These large deviations contrast drastically with those from the TNT-based charges and might correctly be interpreted as a diameter effect, but one that appears to be influenced significantly by the energy consuming characteristics of the polyethylene and aluminum components of the formulation. The limited data generated by this test series and the pre-1988 experiment suggest that D(HBCNQ) may be approaching a maximum value that is medium and crystal habit dependent. D(SNQ), on the other hand, is similar to D(HBCNQ) for similar charge densities up to a charge diameter of only 38.1 mm, where input pressure is that of Composition B. This D(NQ)

similarity persists to a charge diameter of 73.2 mm at a reduced input pressure (39 kbar). Above this input pressure, D(SNQ) increases rapidly to a value similar to that observed in a TNT medium. At a diameter of 175 mm and input pressure of only 35 kbar, ideal behavior is achieved. For this latter case, it is not clear whether or not the ideal performance results from the increased diameter of the charge or the reduced charge density. Again, additional experiments are required to quantify these findings, but it appears reasonable to postulate that the energy-absorbing characteristics of the medium are responsible for the significantly reduced D(NQ) values and to conclude that it is the unique structure of the SNQ spherulite that allows it to overcome the influence of the medium above some diameter d_i.

REFERENCES

1. K. F. Baker, "Thermal Stability of Potentially Hazardous Materials by Differential Scanning Calorimetry (DSC)," DuPont Instruments Application Brief Number TA73, 1970.

2. S. A. Aubert, G. H. Parsons, and G. J. Glenn, Jr, "Calibration and Correlation of a Modified Expanded Large-Scale Gap Test with the Large Scale Gap Test and 8-Inch Gap Test," AFATL-TR-89-46, August 1989, Eglin AFB FL, Distribution limited to US Government agencies only.

3. A. A. Ratcliff, "German Insensitive High Explosive (IHE) Slow Cook-Off and Bullet Impact Tests," MSD-TR-90-20, April 1990, Eglin AFB FL, Distribution Authorized to US Government Agencies Only.

4. Military Standard, "Safety and Performance Tests for Qualification of Explosives," MIL-STD-1751 (USAF), Method 13, 20 Aug 1982.

5. B. M. Dobratz, "LLNL Explosives Handbook, Properties of Chemical Explosives and Explosive Simulants," UCRL-52997, Revised 16 Mar 1984, Chapter 8, Lawrence Livermore Laboratories.

6. D. Price and A. R. Clairmont, Jr., "The Response of Nitroguanidine to a Strong Shock," NOLTR 67-169, 2 Feb 1968, US Naval Ordnance Laboratory, White Oak, Silver Spring MD, Distribution limited to US Government Agencies Only.

INITIAL DISTRIBUTION

DTIC-DDAC	2
WL/MNOI	1
WL/MNME	1